WATER INTERACTION WITH RAW, INTERMEDIATE AND FINAL PHARMACEUTICAL MATERIALS

By

ZHANJIE LIU

A thesis submitted to the

Graduate School – New Brunswick

Rutgers, The State University of New Jersey

In partial fulfillment of the requirement

For the degree of

Master of Science

Graduate Program in Chemical and Biochemical Engineering

Written under the direction of

German Drazer and Gerardo Callegari

And approved by

_____

_____

_____

New Brunswick, New Jersey

October 2020

ABSTRACT OF THE THESIS

Water Interaction with Raw, Intermediate and Final Pharmaceutical Materials

By ZHANJIE LIU

Thesis Director:

German Drazer and Gerardo Callegari

Tablets is the most convenient way to take medication and 70% of the total medicines are dispensed in the form of tablets. The effectiveness of such dosage form depends on how the drug dissolves in the fluids of the gastrointestinal tract. The dissolution of tablets is dominated by two factors mainly: Wettability of the blends and disintegration of the tablets. The objective of this study consists of: A) Studying the wettability of pharmaceutical blends by droplet penetration method. B) Understanding of the Swelling of pharmaceutical tablets in contact with water. In droplet penetration section, blends of 90% Lactose, 9% APAP, 1% MgSt with varying shear level (0Rev, 160Rev, 640Rev and 1280Rev) were prepared as porous material. To characterize wettability of blends, the penetration profile of both water and silicone oil, which is the volume of droplet versus time, was plotted. The water penetration process consists of three phase: bouncing phase, waiting phase and penetrating phase. By reviewing the penetration model developed by Denesuk, a new method for dynamic contact angle calculation was developed. The results reveal that the

wettability of blends decreases as the increasing of shear level. In tablets swelling section, formulations with varying percentage of Avicel and Lactose (80% Avicel-10% Lactose, 45% Avicel-45% Lactose and 10% Avicel-80% Lactose) were used to make tablets with different compaction force ranging from 4KN to 24KN. A experiment was designed to measure the swelling of tablets and mass of water uptake meantime. Both the swelling profile and the water uptake profile of tablets present two behaviors: linear and non-linear, which reveal two possible liquid uptake mechanisms: capillary penetration and particle swelling. Swelling rate and water uptake rate of tablets can be calculated from the swelling profile and water uptake profile. Both of them are non-monotonic with compaction and formulation.

ACKNOWLEDGEMENT

I am trying my best to thank everyone who made my stay and work at Rutgers more wonderful and meaningful.

Foremost, I would like to thank my thesis advisor, Dr. German Drazer and Dr. Gerardo Callegari, for giving me the opportunity to work in pharmaceutical field and encourage me to devote my thesis on it. Their creative suggestions, patient instructions and immense support guided me throughout my research. I would like express my sincere appreciation to my committee member, Dr. Alberto Cuitiño, for his suggestion and feedback.

I would also like to thank the National Science Foundation's Engineering Research Center for Structured Organic Particulate Systems (ERC-SOPS). The faculties and students in this organization provide me invaluable insight to my research. I must particularly mention my colleagues in C6 of C-SOPS, Yifan Wang, Sonia M. Razavi, Golshid Keyvan and Pallavi Pawar, for their insightful discussion, which help me improve my thoughts and ideas in my research. I would like to express my sincere appreciation to Yifan Wang, who has been with me throughout my research on droplet penetration, her motivation and discussion is essential in this project. I would also like to thank Hector Lopez, who is the author of JAVA macro used in the analysis of droplet penetration process and help me to improve my set up for this project.

I would like thank a number of faculties and graduate students that participated in Rutgers University, who enrich my experience in Rutgers and provide insightful discussion, encouragement and friendship. Thank you all for invaluable experience. I am truly appreciated.

TABLE OF CONTENTS

LIST OF TABLES

LIST OF FIGURES

Chapter 1 Introduction

1.1 Motivation

Tablets taken orally gives one of the most convenient means of drug delivery availability. It is the most popular dosage form and 70% of the total medicines are dispensed in the form of tablets. The effectiveness of such dosage form depends on how the drug dissolves in the fluids of the gastrointestinal tract and is absorbed into systemic circulation. Therefore, the rate of dissolution of the tablet is crucial. . Critical Quality Attributes (CQA) includes chemical, physical, biological and microbiological attributes that can be defined, quantified, continually monitored to ensure final product remains in acceptable quality limits. Dissolution profile is one of the most important quality attributes of pharmaceutical products. The profile is usually quantified by the use of some time points (called Q points) and tolerances with respect to those points. The shape of the profile and the location of the Q points usually determine the pharmacological effectiveness of the drug in patients. Dissolution profiles are dependent on both materials and processes. For example, it is well known that the inclusion of a lubricant in minute amounts helps the processing of tablet during the compaction phase, but also that lubricant concentration affects the dissolution profile. On the other hand, for a certain fixed amount of lubricant the dissolution of drug is substantially delayed when mixing time is increased above a certain threshold. Both effects are known as over-lubrication. Approved by the Food and Drug Administration (FDA), dissolution test is sufficient in many cases to build safety and efficacy of pharmaceutical product. The test measures in vitro drug release with time. It is used in the

development of the formulation and tablet processing, as well as in quality control to determine batch-to-batch variability in production.

According to the way the drug is released, tablets are usually classified as: immediate release tablets, extended release tablets and delayed release tablets[1]. The immediate release tablets are formulated to release the active ingredient within a small period of time, typically less than 30min. This dosage forms are designed to provide a fast drug action. The extended release tablets release the active ingredient at a sustained and controlled rate over a period of time, typically 8hours, 12hours and 24hours etc., to reduce the dosing frequency. The delayed released tablets release the active ingredients at a set time. Both the extended release tablets and delayed release tablets are designed to increase the stability, efficacy and safety of drug. In this thesis, we only talk about the immediate release tablets. For immediate release tablets, both the wetting and disintegration of tablets determine the dissolution of tablets. The excellent water wettability of tablet provides faster solvents penetration into tablets and contact with disintegrants. The full disintegration of tablets provides the faster breakdown of tablets into small pieces and releasing active ingredients. In section 1.3, I will discuss the dissolution of immediate release tablet in detail.

1.2 Materials in pharmaceutical product

Drugs or APIs (Active Pharmaceutical Ingredient) are the active ingredients of any pharmaceutical product. Active ingredient means that it has a direct effect on a disease treatment or in its prevention. Other materials, called excipients, are also needed to manufacture the final product. Excipients are the pharmacologically inactive substance alongside the active ingredient of a medication. In direct compressed materials, excipients

work as fillers, binders, disintegrants, glidants and/or lubricants[2-3]. *Fillers* typically are used to bulk up formulations, which make a tablet more practical for users. A good filler not only should be compacted readily but also be inert and compatible with other components in formulation. Lactose, Calcium Carbonate, Glucose, sucrose, Microcrystalline Cellulose are popular fillers. *Binders* are used to hold ingredients together and ensure the tablet can be formed with enough mechanical strength. Binders are typically saccharides derivative, such as Lactose, sucrose, Microcrystalline Cellulose, Maltitol, starches et al. As already mentioned, some compounds my play more than one role, for example, both Microcrystalline Cellulose and Lactose are both fillers and binders. *Disintegrants* facilitate breakdown or dispersion of tablets. When tablets are in contact with water, disintegrants ensure tablets break down into fragments rapidly for quick dissolution and releasing the active ingredients. Examples of Disintegrants include: Polyvinylpyrrolidone, Carboxymethyl Cellulose, Sodium starch glycosylate. *Glidants* improve the flowability of powder during manufacturing by reducing the interparticle cohesion and friction. Examples include: Magnesium carbonate, fumed silica and other silica compounds. *Lubricants* prevent ingredients from clumping together and sticking to manufacturing equipment during the compression of powders into solid tablet. They work as similar action to glidants, however, glidants have no ability to reduce the friction between die wall and particles. Magnesium Stearate, Polyethylene Glycol and Stearic acid are common lubricants.

Lactose and Microcrystalline Cellulose are widely used as excipient in pharmaceutical products. Lactose ($C_{12}H_{22}O_{11}$) is a naturally carbohydrate, found in the milk of mammals. It is a disaccharide composed of one D-galactose and one D-glucose molecule (figure 1.1

A). Due to excellent water solubility, good compressibility properties and cost effectiveness, Lactose is widely used as a filler or filler-binder in tablets and capsules. In water, Lactose swells 10-20% and swells slow. Microcrystalline Cellulose $(C_6H_{10}O_5)_n$ is refined wood pulp, a white and free-flowing powder. It is a polysaccharide composed of glucose units connected by a 1-4 β-glycosidic bond (figure 1.1 B). Microcrystalline Cellulose, which is commonly used in pharmaceutical industry as the filler or binder, has excellent compressibility and dry binding properties. Thus, it is recognized as a direct compression binder[4]. In water, Microcrystalline Cellulose swells and absorbs water very fast. Therefore, in some cases (such as MCC+Lactose), it is considered as disintegrants. Magnesium Stearate, which is the white powder at room temperature, has two long hydrophobic chains (figure 1.1 C). It is FDA-approved inactive ingredient widely used in the pharmaceutical manufacturing to reduce die wall friction.

Acetaminophen, which is a pain reliever and a fever reducer, is used to treat many conditions such as headache, other minor aches, colds and fever (figure 1.1 D). There are two advantages for Acetaminophen (APAP) to be widely used as API in pharmaceutical research: A). Acetaminophen, which has very poor flowability, is a good model for pharmaceutical research. It is used as a material to study the effect of process parameter on pharmaceutical manufacturing. B.) Considering cost effectiveness, Acetaminophen is usually used as the model for other more expensive drugs.

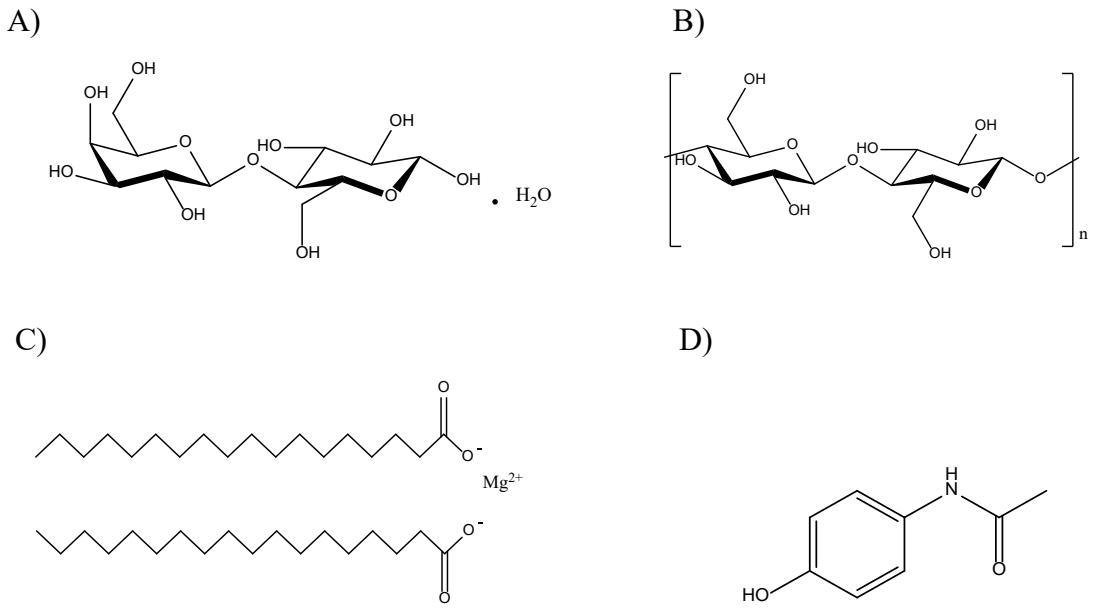

Figure 1.1 Excipients and API: A) α-Lactose monohydrate, B) MCC, C) MgSt, D) APAP

1.3 Dissolution mechanisms of immediate release tablet

The dissolution of immediate tablets consists of three steps: liquid penetrating inside the tablets, the disintegration of tablets, the dissolving of particles.

When tablets are immerged into solvents, liquid penetrates into the tablets through inter-particle pores by capillarity. The penetration of liquid follows Washburn kinetic[5]. Therefore, the solvents penetration rate is determined by porosity and pores sized of the tablets and the wettability of the formulation.

The disintegration of tablets, which is the disaggregation of the compressed tablet into small pieces, play a critical role in drug release. Full tablets disintegration enable the fast dissolution of API, particularly, when the API is poorly water-soluble[6-7]. The disintegration of tablets is the results of a force inside a tablet overcoming several cohesive forces, such as H-bond, electrostatic forces, van der Waals forces etc[8-9]. It seems the phenomenon of the tablet disintegration consists of several processes: swelling of disintegrants, H-bond

annihilation, inter-particle bond weakening, wicking et al. Among those, it is acceptable that the swelling is one of the central mechanism for tablets disintegration because it links to water uptake and force development[10]. In this thesis, we will investigate the dynamic of the swelling and the water uptake with compaction and formulation.

Considering the efficacy of an oral tablets, dissolution of pharmaceutical components, especially the dissolution of API, is crucial because the absorption of the drug occurs only after the dissolving of ingredients. There are two stages in the dissolution process[11]: To dissolve a solid, a liquid molecule must surpass the energy barrier of inter-molecular bond in the solid. Then, the drug molecule must go through the diffusion layer, which is a layer between solid and bulk solution, and diffuses to the bulk solution. There are several elements influence the dissolution of pharmaceutical ingredients: particle size, crystal form, wettability of particle, pharmaceutical factors (the presence of other excipients in tablet).

From the above, the water wettability of formulation and the swelling of tablets are two crucial factors that determine the dissolution of tablets and drug release.

1.4 Blends wettability

Wetting is the ability for a liquid to maintain the contact with a solid. It refers to the inter-molecule interaction between the fluid phase and the solid phase. Wettability, which respects to the degree of wetting, is the tendency of a liquid to spread on a solid surface. It is determined by the balance between the adhesive force and the cohesive force. The Wettability is quantified by the thermodynamic contact angle (θ_T) (figure 1.2) of fluid with the solid via Young's equation:

$$\gamma_{SG} = \gamma_{SL} + \gamma_{LG} \cos\theta_T$$

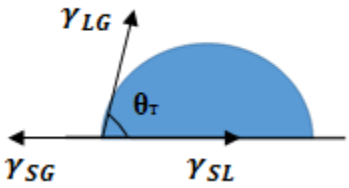

Figure 1.2 Contact angle of a liquid droplet wetted to a rigid solid surface

Where, γ_{SG} is the solid-vapor interfacial energy; γ_{SL} is the solid-liquid interfacial energy and γ_{LG} represents the liquid-vapor interfacial energy. Young's equation is the consideration of a thermodynamic equilibrium between three phases: the solid phase, the liquid phase and the gas or vapor phase. When $\gamma_{SG} > \gamma_{SL} + \gamma_{LG}$, the liquid wets the surface completely. When $\gamma_{SG} < \gamma_{SL} + \gamma_{LG}$, partial wetting occurs. When $\gamma_{SL} > \gamma_{SG} + \gamma_{LG}$, the liquid cannot wet the surface (non-wetting).

Not only for property of final product, blends wettability is also important in pharmaceutical secondary manufacturing, such as wet granulation, impregnation in the fluidized bed and coating in the coating pan etc. The hydrophobicity of blends is determined by both the physical property of raw material (excipient, drug) and the effect of process (blending, lubricating)[12-14]. Most lubricants, which is used to improved blends flowability, are hydrophobic compounds. The concentration of lubricant in blends, such as magnesium stearate (MgSt), affects Hydrophobicity of blends. In addition, studies show the strong impact of shear mixing on blends hydrophobicity[14]. During lubricating process, the lubricant (MgSt), composed of smaller and easily deformed particles, coat on the other

larger and harder particles (Lactose and possibly APAP). Shear rate and strain level in blending process are crucial process parameters[14]. The shear device will be described in chapter2 (section 2.2.1) particularly. Increasing shear in process approaches more homogenous blends. Previous results show, when MgSt is present, wettability of blends decreases with higher shear rate and stronger strain (longer lubricating time)[12-13].

Measuring the wettability of lubricated blends by Washburn column is widespread in powder technology. Washburn reported the phenomenon that liquid rises into the powder bed because of the capillary force[5]. A method of measuring water wettability of powder was developed which measure the speed that a liquid permeates through a column of powder[12-13] (figure 1.3).

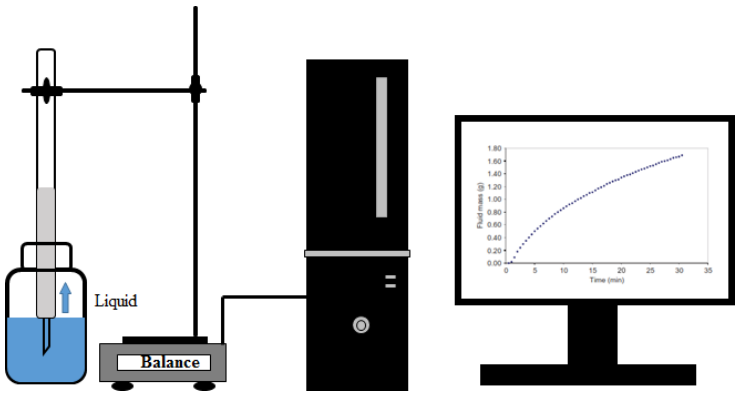

Figure 1.3 Setup of washburn method

The Washburn method can be expressed as the linear function between square of absorbed liquid mass (w^2) and time (t):

$$t = \frac{\eta}{C\rho^2\gamma_L \cos\theta} w^2$$

Where, η is the viscosity of liquid, ρ is the liquid density, γ_L is the surface tension of liquid, θ is the contact angle between solid and liquid, C is the geometric factor, which is constant as long as the packing and the particle size remains similar. Water wettability of blends is defined as the slope of this linear function ($\eta / C\rho^2\gamma_L \cos\theta$).

Droplet penetration is an alternative method that is used to characterize the wettability of the powder material with respect to a liquid. Single droplet is absorbed into the powder bed by capillary pressure. Previously, based on Washburn equation, droplet penetration time was studied by Middleman[15] and used for material characterization in soil science, food science, and pharmaceutical field et al[16-19]. More details about penetration model and previous research can be seen in chapter2 (section 2.3). However, the assumption of Washburn equation is homogeneous capillary path. Previous study found the theoretical droplet penetration time does not correspond to the experimental data in heterogeneous system, which include chemical heterogeneous components[20]. Therefore, in this thesis, not only focus on the penetration time, we also investigate the whole penetration profile that is the volume of droplet versus time.

1.4 Background for tablet swelling analysis

Tablets are made by compaction of blended powder. Compression degree is important in the manufacturing. A tablet must be hard enough to avoid damage in the process of transport, storage, handling and post-processing as coating. On the other hand, compression degree alters disintegration of tablet[21]. During compaction, particle-particle bonds are generated as particles come together and contact closely[22]. Bonding force is corresponding to the strength of the tablet. On the contrary, the disintegration of tablets also includes

several process: swelling of excipients particles, H-bond annihilation, inter-particle bond weakening, wicking etc[9-10]. Understanding the role of these mechanisms and controlling their incidence are essential for tablet design. Tablets made by higher compression degree have lower porosity. In addition, the bonding force between particles increases with compression[21] and disintegration time of tablets correlates with compression. Hence, it is not a surprise that tablets made by higher compression degree have slower disintegration.

Swelling is the volume expansion of a polymeric particle contacting with a solvent due to solvent penetration into the polymeric structure and local re-arrangement of polymeric structure. Therefore, the volume of those polymeric particles increases during the solvent uptake (swelling process)[23]. At the same time, while a particle swells it exerts a pressure on the surrounding particles, which is translated into a swelling force. The role of swelling in disintegration is to provide enough force to disrupt the inter-particle bond[6]. Thus, disintegration of tablets occurs due to the force is exerted on the tablet matrix[24].

In the last 30 years, Caramella and collaborators studied disintegration dynamics and disintegrants swelling[6-8, 10, 25-28]. They characterized the swelling property of different disintegrants and drew the following conclusions: A). No disintegration force is developed if the swelling of the disintegrant is not significant. Moreover, he reported that not all the volume expansion contributes to the development of swelling force[6, 10]. Some disintegrants would have excellent volume expansion, but the disintegration time of tablets made of these disintegrants is long because it doesn't develop much swelling force in the swelling process[6, 10]. Therefore, the ability for a disintegrant to create swelling force is related with its disintegrant efficiency (disintegration time). B). They studied the relationship between the amount of disintegrants and the disintegration force development[6]. They reported, in

the case of highly swelling material, the force transmission of pure disintegrants is hindered. Therefore, the swelling force does not increase with the amount of disintegrants monotonically. We can say the swelling behavior of disintegrant particles in tablets is strongly affected by surrounding particles. During Caramella's research, they also developed an apparatus to measure the disintegration force[25-26], which is the first to measure force development in disintegrating process.

When the filler is α-monohydrate Lactose (water-soluble) and the disintegrant is Microcrystalline Cellulose, Caramella and co-authors acknowledged that the water penetration rate, rather than the disintegrating force development rate, becomes the dominant factor in the disintegration process[10]. They drew the conclusion that, in this case, the passive mechanisms (such as dissolution or H-bond annihilation) seems to prevail over active mechanisms (developing a disintegrating force). In addition, the measurement of water penetration provides a better understanding of disintegration properties.

Actually, Barry and Ridout reported the non-monotonic behavior of disintegration with tablets compaction in 1950[21]. By measuring disintegration time, a critical compression was observed which gave minimum disintegration time. Barry and Ridout relate the disintegration of tablet with starch grains swelling. For light-compression, starch grains didn't exert pressure on surrounding granules immediately during the swelling process duo to large intergranular spaces. Thus, disintegration time is long. For highly compressed tablets, time is required for water to go thought outer layer of tablet before swelling. Only in critical compression case, grains exert pressure on surrounding granules rapidly and tablets break into pieces.

We mentioned dissolution test is useful to characterize tablets. However, the standard test cannot provide insight in the disintegration and liquid penetration mechanisms. In goal of studying tablets disintegration, we designed quantitatively measurements to understand these mechanisms. The tablets swelling profile and the water uptake profile were established, which makes swelling dynamic measurements be possible

Chapter 2 Droplet Penetration on Heterogeneous Powder Bed

As a method of material characterization, droplet penetration technique was developed in many filed, such as water repellency in soils, rehydration of food powder (milk, coffee and cocoa drink) and wet granulation process et al. There are many studies correlating the wettability of material with droplet penetration time[16, 20]. However, no published literature is showing the penetration profile, which is the volume of droplet versus time. In this chapter, we use droplet penetration technique to characterize the wettability of different pharmaceutical blends: pure Lactose, blends of Lactose+APAP with different shear level and blends of Lactose+APAP+MgSt with different shear level. Not only penetration time, the whole penetration profile will also be performed. The process of water droplet penetration depends on chemical property (wettability) of material significantly. Therefore, it is possible to detect the wettability of material using droplet penetration technique However, we cannot ignore the effect from porosity of powder bed and pores radius on droplet penetration. To make our results independent from the pore geometry, the penetration behavior of silicon oils with different viscosity, which have excellent wettability, are performed. We will also review droplet penetration model developed by Wenzel, Cassis and Baxter, Marmur and Denesuk to understand the penetration dynamic. Then, a new method for calculation of dynamic contact angle will be derived from penetration model.

2.1 Materials and Methods

2.1.1 Porous structure Characterization

The Formulation was made by mixing several pharmaceutical powders, which includes excipient (α-Lactose monohydrate), active pharmaceutical ingredient (semifine Acetaminophen (APAP)) and lubricant (MgSt). Powder properties are summarized in Table 2-1.

Table 2-1. Particle size of raw material

Material	Mean(μm)	d10(μm)	d50(μm)	d90(μm)
α-Lactose monohydrate	71.9	10.3	63.5	157.7
Semifine Acetaminophen	48.9	5.6	32.6	122.7
MgSt	8.8	2.1	7.8	16.6

Formulation of 90% Lactose, 9% APAP and 1% MgSt was mixed in V-blender. The capacity of V-blender is 1Kg. 700g Lactose and 70g APAP were added in V-blender (figure 2.1 A) without intensifier bar first for 15min blending. After that, 7.78g MgSt was fed in V-blender for another 2min. Shear effect was added to the blend in a controlled way by using modified Couette shear cell (figure 2.1 B) which is a high shear mixer with controllable shear rate[1]. This device includes two concentric cylinders; the external is stationary while the internal rotates at a pre-fixed rotational speed between 1 to 245 RPM. The gap between cylinders has a total volume of 0.6l, and we fill it with 150g of blend which occupies approximately 0.3l. Both internal and external cylinders have interlocked pins to make sure that all the shear fields are homogenous. Blends with varying wettability can be achieved by different lubricating time in Couette shear cell[14]. Shear rate was fixed at 80Rev/min and 150g blends was fed into shear cell. As exposed strain increase, four blends with different shear level were obtained: 0Rev, 160Rev, 640Rev and 1280Rev.

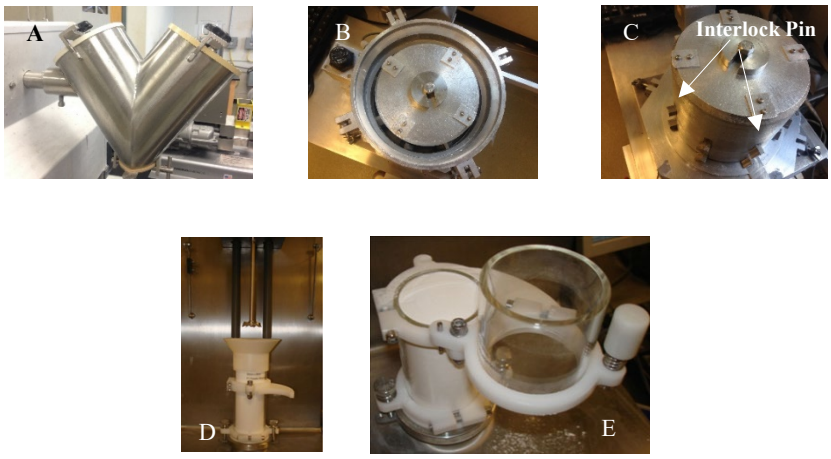

Figure 2.1 Device for blending and powder bed: A). V-blender B). Couette shear cell C). Inter cylinder of Couette shear cell D). FT4 powder rheometer E). Powder bed

Properties of these four blends are shown in figure 2.2. Particle size distribution was measured using a Laser Diffraction Spectroscopy technique (Beckman-Coulter LS 13 320 series laser diffraction particle size analyzer). From figure 2.2 A, the particle size distribution doesn't represent any difference with shear. Bulk density (figure 2.2 B) is calculated as the dry weight of powder (or granular solid) divided by its volume. This volume includes the volume of particles and the volume of pores. Bulk density is not the intrinsic property of particles, it depends on how closely they are packed. Tapped density (figure 2.2 C) depicts the bulk density of powder (or granular solid) after consolidation or compression. The method of tapping is used to achieve consolidation, it is regarded as "lifting and dropping". 20g blends were fed into a graduated cylinder and measured the volume of blends, bulk density can be calculated as mass/volume. Then, the graduated cylinder with blends was tapped 1250 times. After measuring the volume of blend again, the tapped density can be calculated mass/volume (after tapping) as well. True density of particulate solid is the density of particles that make up the powder; it doesn't depend on the degree of compaction of powder. In our case, true density can be expressed as:

$$\rho = f_{Lactose}\rho_{Lactose} + f_{APAP}\rho_{APAP} + f_{MgSt}\rho_{MgSt} \quad [1]$$

$\rho_{Lactose}$, ρ_{APAP} and ρ_{MgSt} are corresponding to density of Lactose, APAP and MgSt. $f_{Lactose}$, f_{APAP} and f_{MgSt} represent the mass fraction of each component. Bulk density and tapped density are smaller than the true density of the powder due to the existence of inter-particle pores. And, Bulk density is smaller than tapped density.

A:

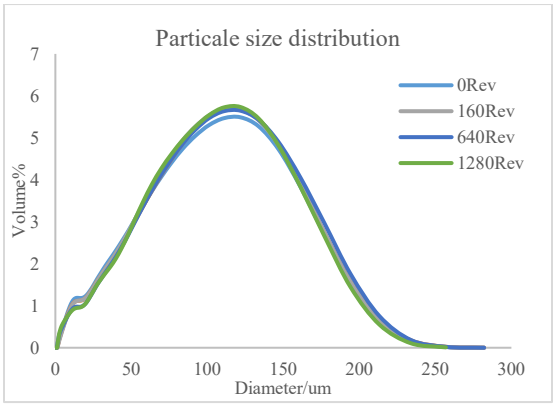

B:

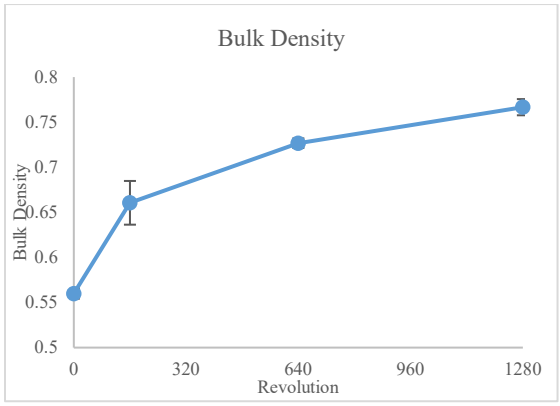

C:

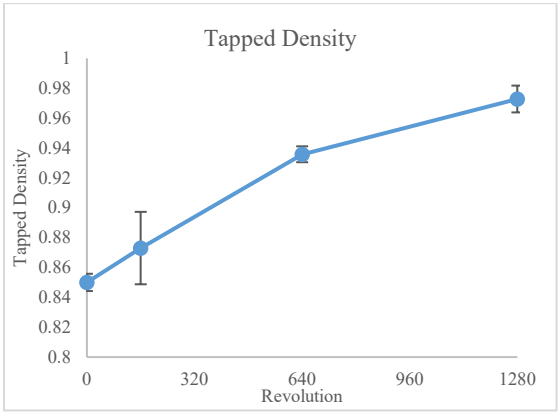

D:

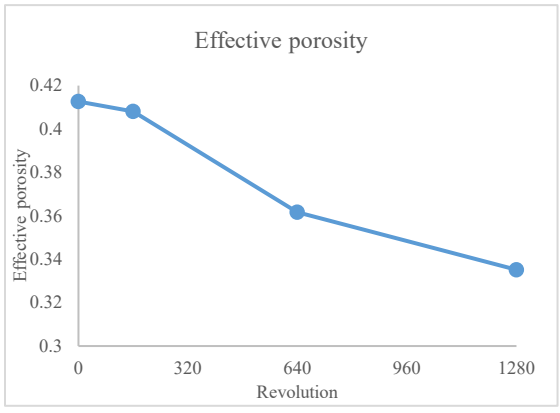

Figure 2.2 Blends properties: A) Particle size distribution. B) Bulk density. C) Tapped Density. D) Effective porosity of powder bed.

We also mixed blends with formulation of 90% Lactose (700g), 10% APAP (70g) and prepared in a modified Couette shear cell for two lubrication level 0Rev and 1280Rev, which are used to compare the penetration behavior of blends with and without MgSt.

Experiments were designed to drop single droplet on a powder bed. The vessel for powder bed is 25mm diameter and 20mm deep. Powder bed was prepared using FT4 powder rheometer (figure 2.1) in three steps. Firstly, the powder was conditioned by a blade to make a powder with higher uniformity (figure 2.1 D). Secondly, the powder in the vessel was compressed by a piston and the compression pressure is 15Kpa. Then, the compressed powder bed was scraped to produce a flat and smooth surface (figure 2.1 E).

The porosity of powder bed was calculated by:

$$\varepsilon = 1 - \frac{m}{\rho V} \qquad [2]$$

Where, m is mass of powder bed, V is volume of powder bed, ρ is true density of formulation. True density (ρ) was calculated from formulation (Eq. [1]): 90% Lactose (density is 1.5588g/cm^3), 9% APAP (density is 1.2294g/cm^3) and 1% MgSt (density is 1.04g/cm^3)[29].

Hapgood et al. (2002) studied drop penetration time and wicking behavior. They introduced effective porosity (ε_{eff}) due to the observation of macrovoids in powder beds[16]. The presence of macrovoids will prevent the liquid penetration due to the penetration path suddenly widen. The sudden widening decrease curvature of the liquid and driven force of penetration and halt liquid flow. Effective porosity, which eliminate the effect of macrovoids, relates to powder bed voidage (ε) and tapped voidage (ε_{tap}) (Eq. [3]). As

shear level increases, effective porosity of powder decreases due to achieving a more homogenous blends (figure 2.2 D).

$$\varepsilon_{eff} = \varepsilon_{tap}(1-\varepsilon+\varepsilon_{eff}) \quad [3]$$

2.1.2 Droplet penetration technique for wettability characterization

In last section, we mentioned different process parameter (level of strain) also gives the difference of bulk density, which means the structure of powder bed is different with shear level. Therefore, the penetration behaviors of silicone oils with different viscosity are performed to remove the effect of pore geometry. Liquid properties are summarized as table 2-2.

Table 2-2: Property of liquid

Liquid	Kinematic viscosity/cst	Density g/cm^3	Surface tension mN/m
DI water	1	1	72.8
Silicon oil 1	3	0.898	19.2
Silicon oil 2	10	0.935	20.1

The droplet penetration behavior was studied by analyzing the volume of droplet versus time. 1cc/ml syringes and needles with 0.5mm diameter were used to drop single droplet on powder bed from a controlled height. Droplet size of water, 3cst silicone oil and 10cst silicone oil are 9µl, 2.69µl and 2.99µl. A CCD camera (AVT Gige camera) and StreamPix6 video recorder were used to capture the droplet penetration process. The frame rate of camera was set to 58 frames/s, which allows the camera capture more details of penetration process. Exposure time of camera was set to 300µs, which allows the camera has faster shutter and can capture the momentum of droplet clearly. Droplet penetration set up is shown in figure 2.3.

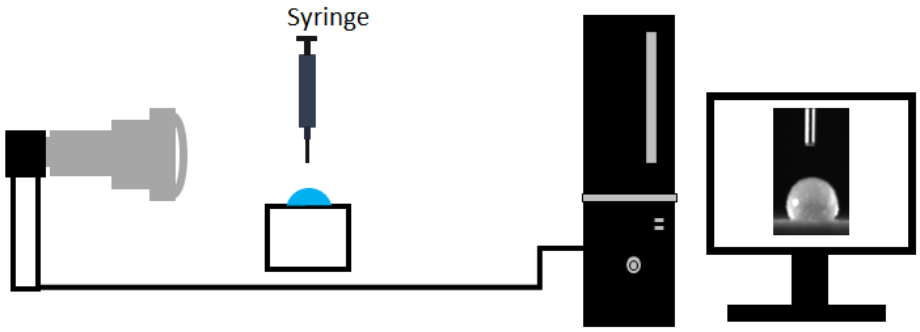

Figure 2.3 Droplet penetration experiment setup

At least 5 replicates and 2 powder beds were performed for each blend and each liquid. To make sure that the penetration path of droplet does not overlap with each other, less than 4 droplets were dropped on one powder bed, and the distance of more than 1.5cm was performed between 2 droplets. The gap between bottom of needle and upper surface of powder was kept at 5mm to ensure similar and small momentum at impact. ImageJ[30], an open source and freeware software created by the NIH, was used to analyze video. ImageJ subtracts the background from each image, applies an automatic threshold, binarizes the stacks. A simple macro was developed in the group to calculate the volume of droplet in each frame assuming the droplet is axi-symmetric. Therefore, volume of droplet as a function of time was measured.

2.2 Droplet penetration experiments

Both the physical properties of raw material and process condition (shear rate and level of strain etc.) impact the property of final product (tablet or capsule)[12-13]. In this section, we will show the droplet penetration behavior of pure Lactose; blends of Lactose and APAP; blends of Lactose, APAP and MgSt to investigate how the raw material affect wettability of blends. On the other hand, droplet penetration behavior of blends with varying shear

level shows the effect of shear level on wettability of blends. We just investigate the penetration behavior of 10cst silicone oil for pure Lactose and blends of Lactose and APAP. There are two reasons for that: A). the similar results of contact angle calculation were obtained between 10cst silicone oil and 3cst silicone oil, which we will show in section 2.3.2. B). Due to larger viscosity, longer penetration curve would be obtained.

2.2.1 Penetration behavior of pure Lactose

Penetration process of water and 10cst silicone oil are shown in figure 2.4.

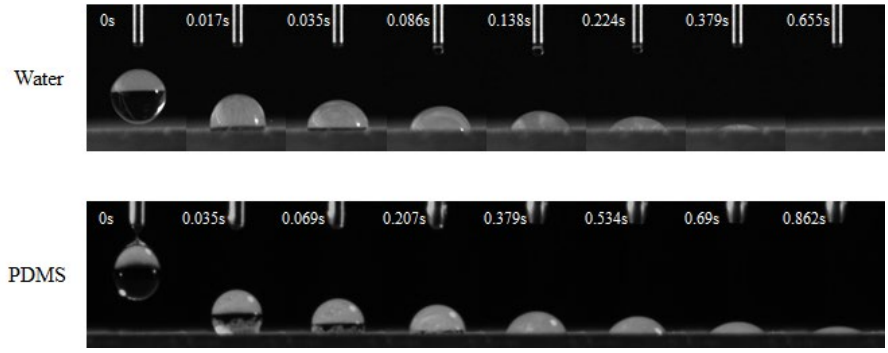

Figure 2.4 Penetration process of water and 10cst silicone oil on Lactose

When both water and silicone oil touched on powder bed, liquid was drawn into pores in less than 1 second. Figure 2.5 presents penetration profile of water and silicone oil. Comparing penetration time, 10cst silicone oil is longer than water even the droplet size of water (9µl) is much larger that silicone oil (2.99µl), which reveals that, in this case, the effect of viscosity on penetration process becomes dominant instead of the effect of wettability.

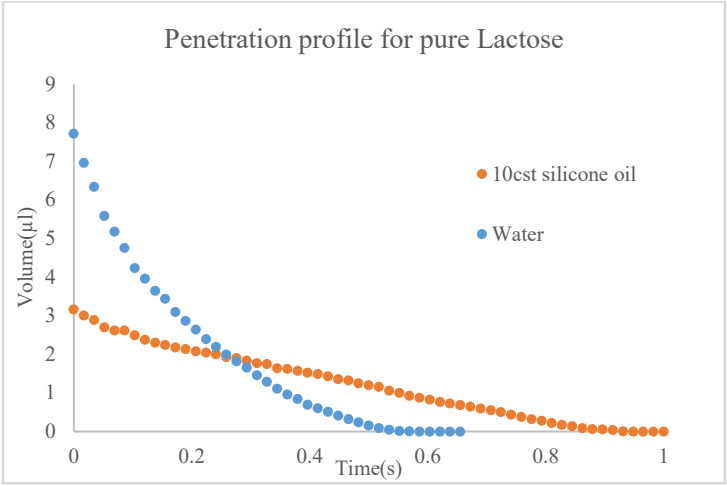

Figure 2.5 Penetration of water and silicone oil on Lactose

2.2.2 Penetration behavior of formulation with Lactose and APAP

Penetration processes of water and 10cst silicone oil are shown in figure 2.6.

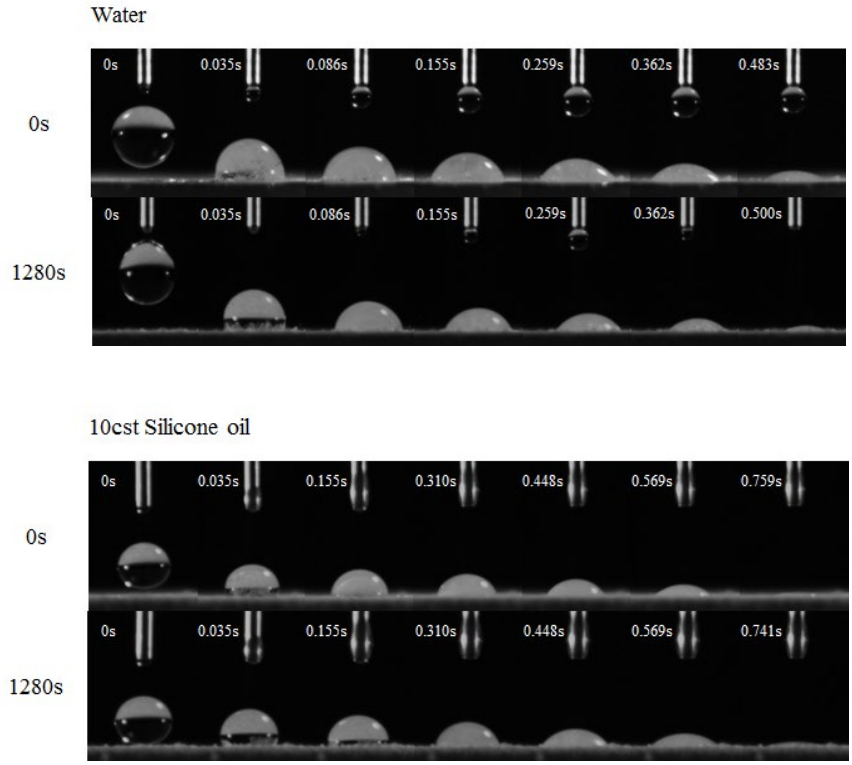

Figure 2.6 Penetration process on Lactose+APAP

Liquid was imbibed into powder bed immediately. When water droplets touched the powder bed surface, particles attached on droplets surface. From section 2.1.1, we know Lactose particles doesn't coat on droplet since Lactose particles can dissolve into water easily. Thus, these coated particles should be APAP particles, which need more time to dissolve into droplet. This phenomenon reveals that Lactose is more hydrophilic than APAP. Penetration profiles were plotted in figure 2.7. Penetration behavior of both water and silicone oil have no appreciable difference between 0Rev blends and 1280Rev blends. Therefore, it looks shearing has no effect on wettability of blends without MgSt. Furthermore, porosity and pores size of the powder bed without MgSt don't depend on the shear condition as well. Longer penetration time of Silicone oil in both 0Rev and 1280Rev attributes to larger viscosity of Silicone oil, which reveal that the effect of viscosity on penetration process becomes dominant instead of the effect of wettability.

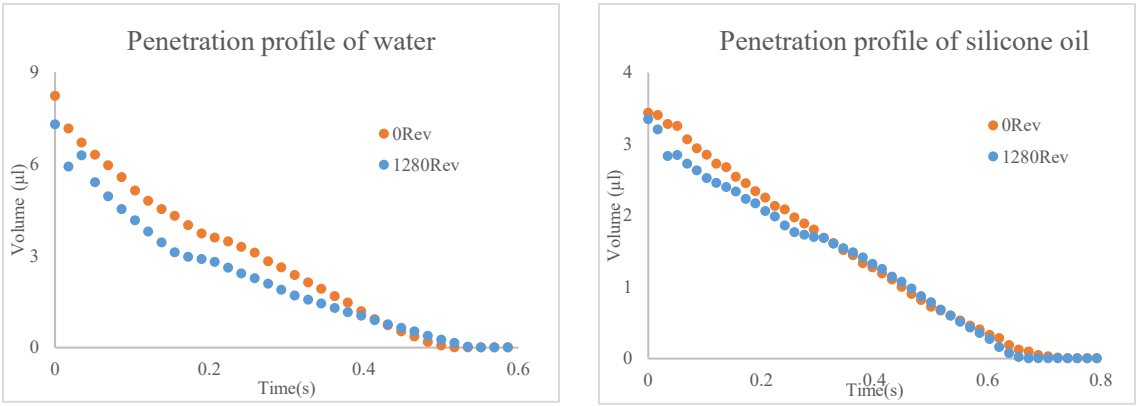

Figure 2.7 Penetration profile on Lactose+APAP

2.2.3 Droplet penetration behavior of formulation with Lactose, APAP and MgSt

A sequence of the water droplet penetration processes can be seen in figure 2.8. Three phases in penetration process were found.

A) Bouncing phase.

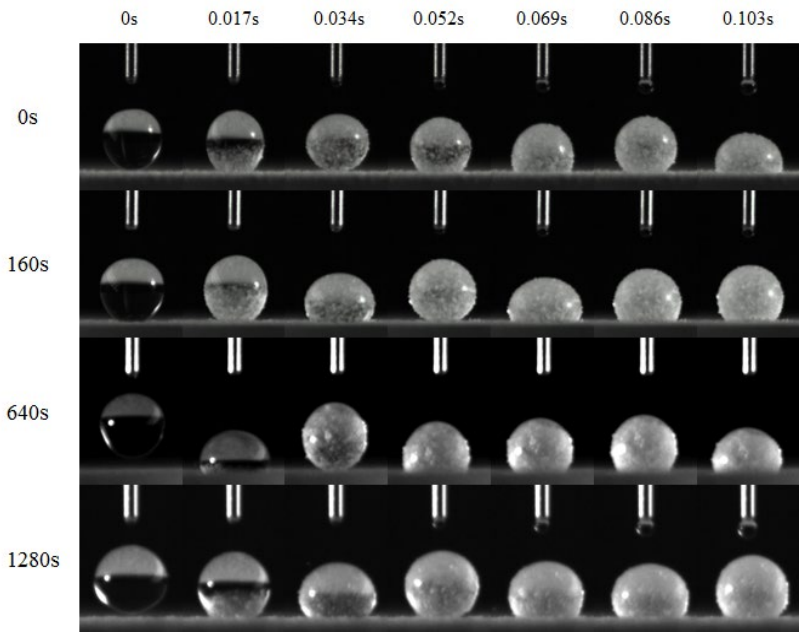

B) Waitting phase

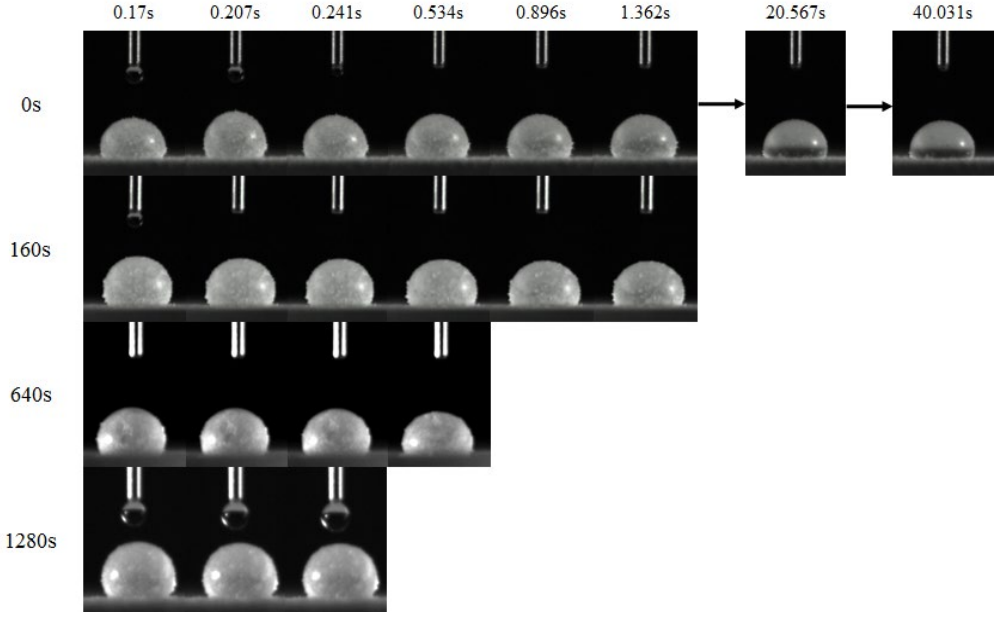

C) Penetrating phase (set the penetrating phase start from time 0s):

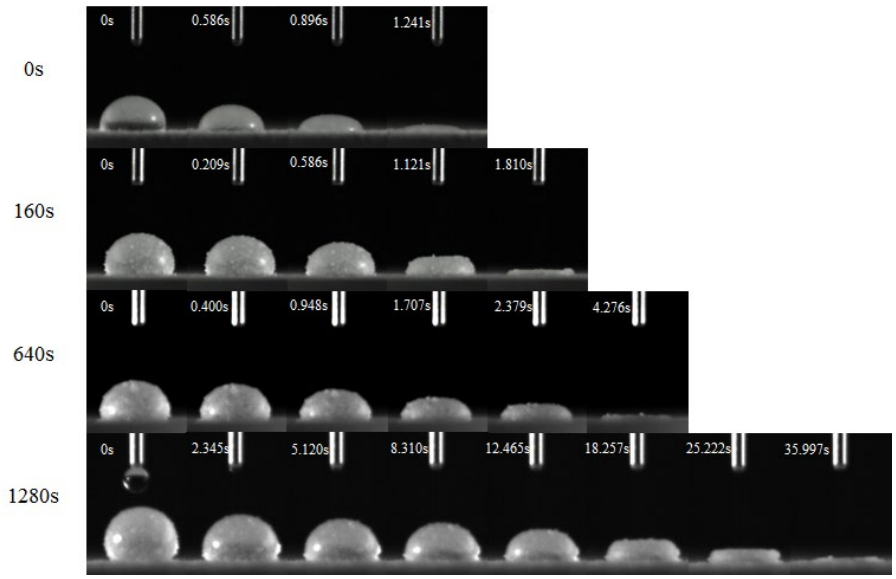

Figure 2.8 Phases of the water droplet penetration process in powder beds of blends with different shear level

Volume of droplet as function of time was plotted in figure 2.9.

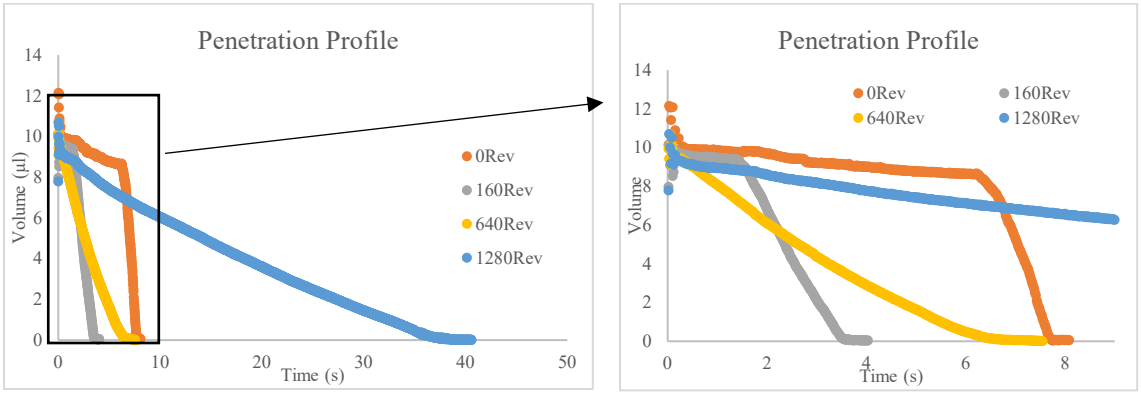

Figure 2.9 Penetration volume with time

After droplet touching on powder bed, three phases were observed in penetration process:

- A) Bouncing phase. When the droplet touches the upper surface of powder bed, it bounces up and down probably due to the momentum of droplet. In the bouncing phase, droplet accommodates and collects particles from powder bed surface. From section 2.2.1 and 2.2.2, we know that Lactose doesn't attach on droplets due to

excellent water solubility. In addition, APAP always attaches on droplets. Thus, we can conclude that these attached particles are APAP and MgSt. With increasing level of strain, the lubricant (MgSt), composed of smaller and easily deformed particles, coat on the other larger and harder particles (Lactose and possibly APAP). Therefore, it is not surprising that Lactose and APAP particles form a hydrophobic film for blends with high shear level. From figure 2.8, more particles attach on the droplet with level of strain. Fluctuation in the beginning of penetration curves are probably due to droplet not being axi-symmetric during bouncing. Also, a cushion of air is created that prevents liquid from being in direct contact with inner layers of the powder bed. Time is needed for the droplet to be pinned on the the powder bed.

- B) Waiting phase. When droplet is pinned on powder bed, it stays on the powder without penetrating for a certain time. We call this the waiting phase. Our observation reveals an a-priori counter-intuitive result that waiting time decreases with level of strain (figure 2.10). Obvious waiting phase exists in 0Rev and 160Rev blends, and no waiting phase is observed for 1280Rev. Limited spreading of solid-liquid contact line was observed in waiting phase.

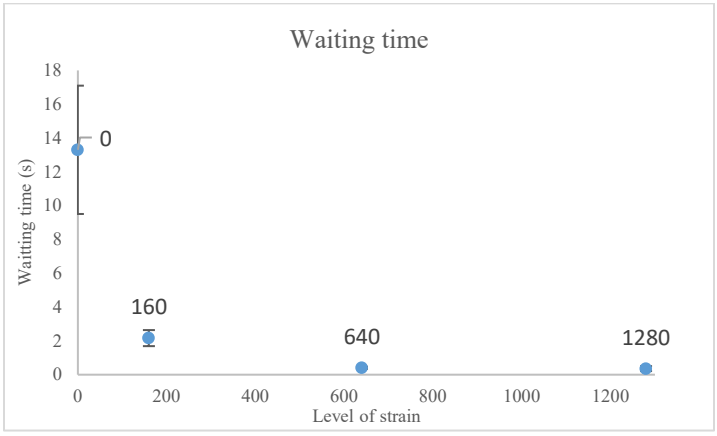

Figure.2.10 Waiting time of blends with different shear level

Moreover, different waiting time was found in same blends. In the experiments of 0Rev blends, the waiting time vary at the range from 3s to 57s. The difference of waiting time leads to different total time (figure 2.11). Therefore, we cannot regard the total time as droplet penetrating time simply.

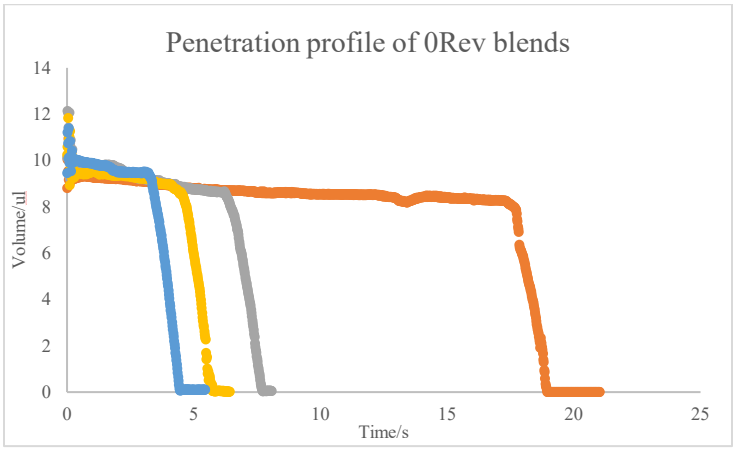

Figure 2.11 Penetration profile of 0Rev blends

- C) Penetration phase. When the liquid reaches the hydrophilic particles, it penetrates into the powder bed. The penetration phase is related to wetting properties of materials and the porous structure: pore size distribution, pore connectivity and geometry. There is another observation: during the penetrating

process of 160Rev, 640Rev, 1280Rev blends, the shape of the droplets stays spherical cap initially and the external contact angle between solid and liquid decreases continuously. However, sometime later, the external contact angle and contact area between liquid and solid stay constant. The top surface of droplets falls down, meaning the height of droplet decreases (for example, frames of 18.257s and 25.222s of 1280Rev in figure 2.8 C). To compare penetration behavior of blends with different shear levels, the penetration profile in penetrating phase was plotted in which the bouncing phase and the waiting phase were removed (figure 2.12). From the penetrating phase profile, longer penetrating time was observed obviously for larger shear blends, which may indicate more hydrophobic blends. As said before, absorption time is not uniquely related to wettability as the porous material structure matters. We will discuss later how to separate both contribution by using a different liquid.

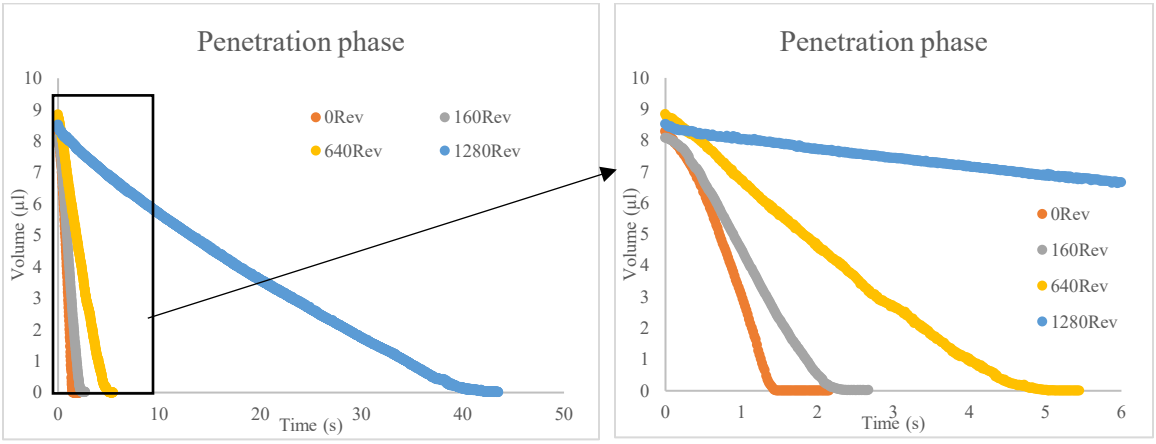

Figure 2.12 Penetration curve in penetration phase

Porosity corresponds to the number of liquid penetration path. Therefore, the droplet penetration process also depends on porosity and pores size of the powder bed. To remove the effect of powder structure on penetration behavior, silicone oils, which have low

surface tension and wet most surfaces, was used. Thus, only the powder physical structure determine penetration behavior of silicone oil as contact angle between the liquid and our materials is zero. Two silicone oils with different viscosities 3cst and 10cst were used for characterization. Penetration processes of two silicone oils on 640Rev blends are shown in figure 2.13.

A: 3 centistokes silicone oil, 640Rev

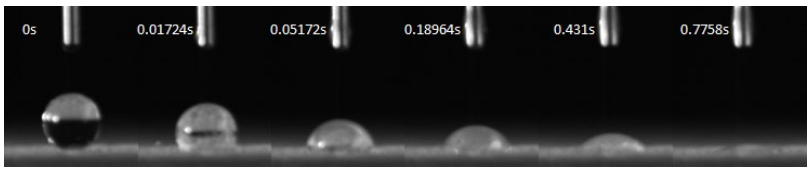

B: 10 centistokes silicone oil, 640Rev

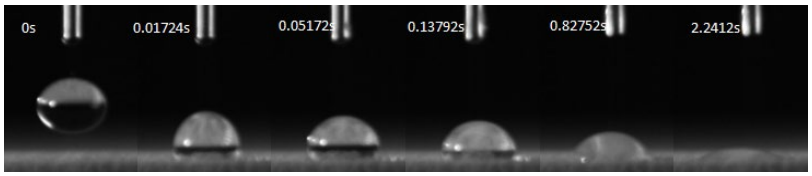

Figure 2.13 Silicone oil penetration process

No bouncing or waiting phases were observed within the silicone oil droplets penetration and particles didn't attach on droplets. When droplets were dropped on the powder bed surface, liquid penetrated into the powder bed immediately. The penetration profile (figure 2.14) shows penetration dynamics of the four blends for both silicone oils. The penetration time of 640Rev and 1280Rev blends are longer than 0Rev and 160Rev blends, which is the results of smaller porosity of 640Rev and 1280Rev (figure 2.5 D). Furthermore, longer penetration time of 10cst silicone oil was observed on all blends than 3cst silicone oil.

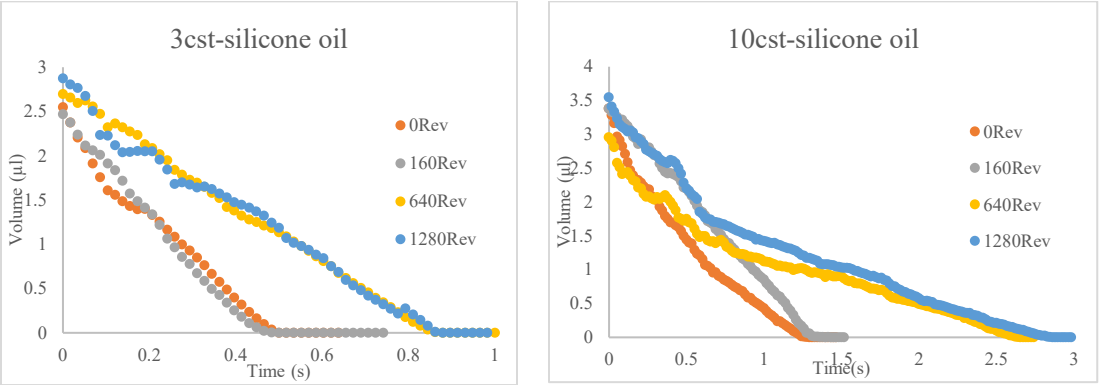

Figure 2.14 Penetration curve of silicone oil

2.3 Analysis and Discussion

2.3.1 External contact angle and waiting phase:

The wettability of a material with respect to a liquid can be obtained from measuring the external contact angle, which is the tangent angle between the solid-liquid interface and the liquid-vapor interface. Contact angle on surfaces does not depends solely on the wettability as the roughness also affects it strongly. Wenzel[31] proposed to relate the thermodynamic (Young's) contact angle θ_T with the measured (external) contact angles θ_e through roughness (r) of the surface in the following equation (figure 2.15 B). Wenzel's theory is described by the equation:

$$\cos\theta_e = r\cos\theta_T \qquad [4]$$

Another type of description of the wettability on surface is a corollary of Cassie and Baxter's description of the contact angle of a composite material[32]. The modified Cassie-Baxter model describes the external contact angle on a heterogeneous and porous material. When the droplet sits on a chemically heterogeneous surface with component 1 and 2, the

surface protrusions and the air beneath droplet support liquid (figure 2.15 C). The external contact angle can be expressed by the equation:

$$\cos\theta_e = \varphi_1 \cos\theta_1 + \varphi_2 \cos\theta_2 - (1 - \varphi_1 - \varphi_2) \quad [5]$$

Where, θ_e is external contact angle; φ_1, φ_2 are area fraction of component 1 and component 2; θ_1, θ_2 are intrinsic contact angle of component 1 and 2; $(1- \varphi_1- \varphi_2)$ represents area fraction of air.

The rough surface contains lots of the protrusions. Therefore, the Cassie-Baxter situation always happens before the Wenzel's. In our case, the loose powder bed gives very rough surface and large porosity, and MgSt particles form hydrophobic surface protrusions. Thus, when droplet sits on powder bed, Cassis-Baxter state approaches. However, Cassie-Baxter situation is metastable and any vibration helps the system to decay into Wenzel's state, which is a pre-requisite for droplet penetration when the material is composed by liquid-phobic and liquid-philic materials.

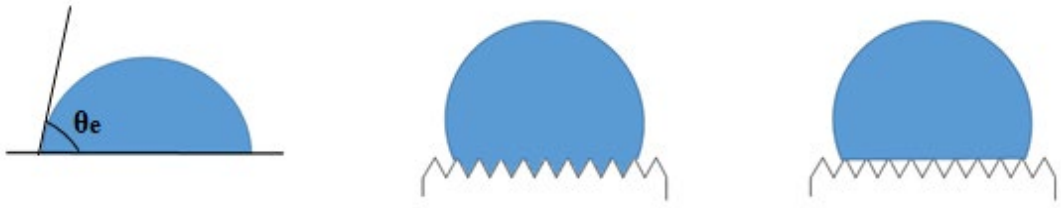

A. B. C.

Figure 2.15 Description of droplet on material surface: A) Smooth surface, B) Wenzel type, C) Cassie-Baxter type.

We hypothesize that the less the material is sheared, the higher the hydrophobic protrusions are and the farther the liquid is from the hydrophilic granules which, we think, is the reason why the less sheared blends display longer waiting times. More work is needed to clarify this hypothesis. As the shear level increases, more MgSt particles attach on the surface of

Lactose, more homogeneous powder bed surface can be produced. Therefore, large waiting time distribution (from 3s to 57s) was observed for the no-shear blends (0Rev), due to the large heterogeneity of blends.

Assuming the spherical cap shape of droplet on powder bed, the external contact angle can be calculated by measuring the height of droplet (h) and the radius of contact area (r). The expression is:

$$\cos\theta_e = \frac{r^2 - h^2}{r^2 + h^2} \quad [6]$$

The external contact angle versus time of four blends with different shear level were shown in figure 2.16 A.

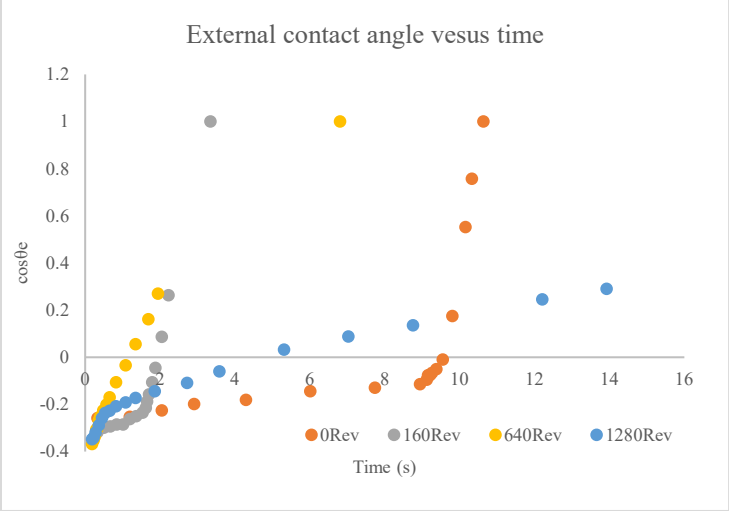

Figure 2.16 External contact angle

During the water penetration process of pure Lactose, Lactose+APAP, 0Rev of Lactose+APAP+MgSt, the external contact angle always decreases until all the liquid is imbibed into powder bed. However, the contact area of them goes through three stages: spreading, constant area, drawing back. An example of 0Rev-Lactose+APAP+MgSt can be seen in figure 2.17, the contact radius between water droplet and solid spreads from

1.28mm to 1.38mm initially, and then, stays constant. Sometime later, it draws back from 1.38mm until the liquid is imbibed into powder bed. In the case of 160Rev, 640Rev, 1280Rev, both external contact angle and contact area increase at first. Then, they are constant until the liquid finishes penetration. Figure 2.18 shows the external contact (cosθ) versus the change of contact radius from maximum value (Δr).

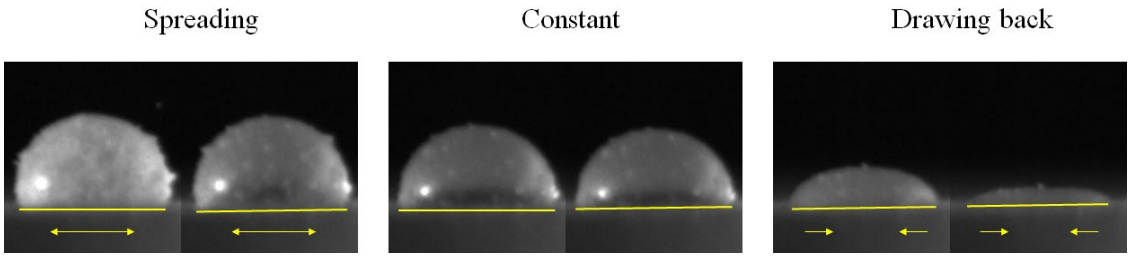

Figure 2.17 Three stages in penetration process of 0Rev-Lactose+APAP+MgSt

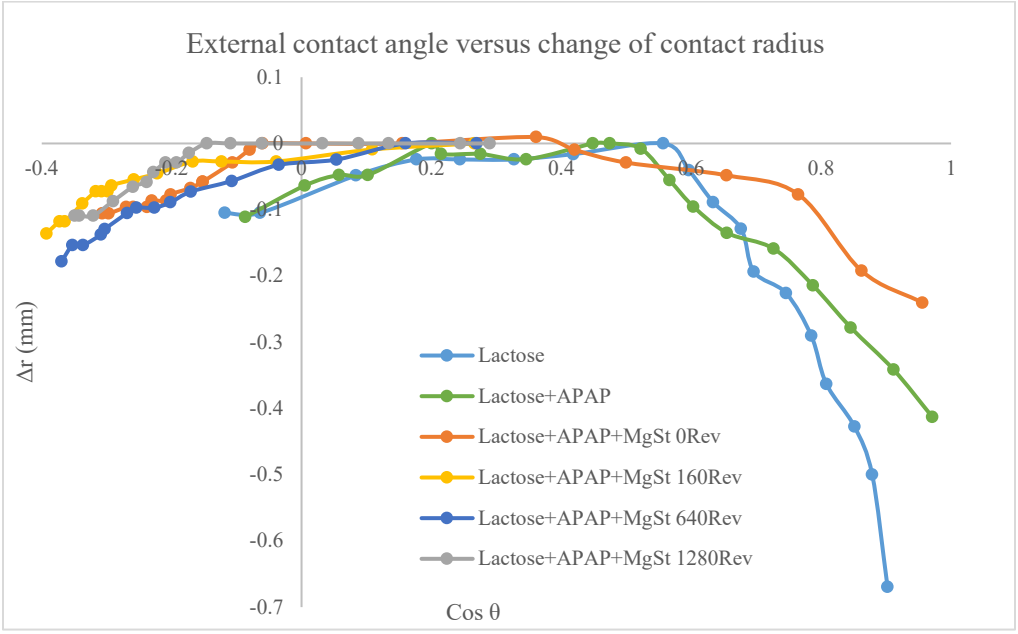

Figure2.18 Relationship between external contact angle and radius of contact area

2.3.2 Penetration Model review:

Droplet penetration dynamics was studied for a very long time. In 1988, regarding the external contact angle of droplet, behavior of liquid droplet and radius of droplet curvature,

Marmur[33] defines two limit cases for droplet penetration simplifying the much more complex real behavior. He assumed the radial capillary is two parallel, rigid and nonporous plate (figure 2.19). One of the plates has a small hole. The first case is constant drawing area (CDA) case (figure 2.20 A). During the penetration process, the contact line of liquid-solid remains stationary, the contact line is said to be “pinned” in this case. The external contact angle of droplet decreases while the droplet is being imbibed by porous material. The droplet external contact angle decreases with penetration as the volume of droplet decreases and the area in contact with the porous material is fixed. Constant contact area ensures that the number of pores beneath droplet is constant. The other limiting case is decreasing drawing area (DDA) case (figure 2.20 B). In the second case, it is assumed that the apparent contact angle remains constant while the contact line recedes on the substrate and liquid penetrates into the porous material. There is no fundamental reason why the contact angle should remain constant while the contact line retracts on the surface of the porous material, it is just and ad-hoc assumption to simplify the problem.

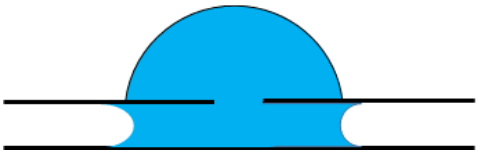

Figure 2.19 The radical capillary penetration model

A B

Figure 2.20 Two limit case: A). constant drawing area. B). decreasing drawing area.

Most of the times a real experiment is more complex that these simplified descriptions, however they may be used to explain at least part of the full dynamics. The real situation is bound between these two limiting cases.

Porous material is modeled as parallel cylinders with solid walls[34]. The cylindrical pores are assumed as infinite depth with the radius R, and the number density per unit area ρ_p (figure 2.21 A). Surface energy represents the work per unit area, which disrupts the intermolecular bond when a surface is created. For liquid, the surface tension (force per unit length) and the surface energy density (surface energy per unit area) are identical. When the surface energy of solid-liquid (γ_{sl}) is smaller than the surface energy of solid-vapor (γ_{sv}), the replacement of the solid-vapor interface by the solid-liquid interface will be favorable. Liquid can be imbibed into pores by capillarity.

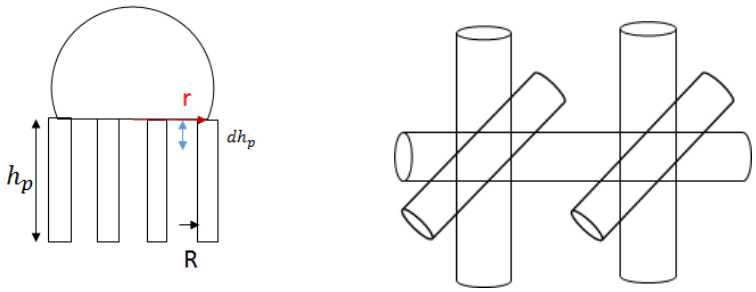

A. B.

Figure 2.21 Penetration model: A) Porous material geometry B) interconnected pore geometry

The Penetration pressure can be represented by the change of free energy per volume of liquid imbibed into pores:

$$\Delta P = \frac{\partial F}{\partial V} = \frac{(\gamma_{sv} - \gamma_{sl}) \cdot 2\pi R dh_p}{\pi R^2 dh_p} = \frac{2(\gamma_{sv} - \gamma_{sl})}{R} = \frac{2\gamma_{lv}\cos\theta}{R} \qquad [7]$$

Comparing with droplet size, the radius of pores is very small. Therefore, the droplet curvature and the gravitational induced pressure are negligible with respect to the capillary pressure. Assuming pores are infinite depth, the liquid penetrates perpendicularly to the porous surface. Washburn[5] related the penetration depth (h_p) with the penetration time (t) for capillaries with contact angle θ and pores radius R by assuming Poiseuille flow in the straight capillary tube with the pressure head given by capillary pressure due to Laplace. The expression of Washburn equation is:

$$h_p^{\,2} = \frac{\gamma_{lv} R \cos\theta}{2\mu} \cdot t \qquad [8]$$

Assuming the droplet is radical symmetry with radius of contact area (r) and considering the constant drawing area, the total penetration volume can be expressed (Eq. [9]).

$$V_p = c\int_0^t \int_0^r \frac{r}{\sqrt{t'}} dr dt' = \frac{cr^2}{2}\int_0^t \frac{1}{\sqrt{t'}} dt' = cr^2\sqrt{t} \qquad [9]$$

Where

$$c = \pi \cdot \pi R^2 \rho_p \sqrt{\frac{\gamma_{lv} R \cos\theta}{2\mu}} \qquad [10]$$

Porous material always has some degrees of pore connectivity[35-36]. This connectivity increases the rate of penetration by increasing the penetration path. The interconnected pore geometry was shown in figure 2.21 B. The traditional ways to consider pore connectivity is the using of permeability (k)[35], which is the ability for a porous material to allow fluid to go through it. Permeability (k) relates with the pore size (R) and the number

density per unit area of pores (ρ_p)[34] as $k = \pi R^4 \rho_p / 8$. Therefore, Eq. [10] can be replaced to consider the effect of pore connectivity:

$$c = \frac{8\pi k}{R^2}\sqrt{\frac{\gamma_{lv} R\cos\theta}{2\mu}} \quad [11]$$

2.3.3 Absorption time

Absorption time is the time required for the total volume of the droplet to be imbibed into the porous material. Previously, people investigated the droplet absorption time to characterize the hydrophobicity of material. In this section, we will review the droplet penetration time, which was derived from the penetration model[15]. In constant drawing area (CDA), Assuming droplets have the spherical cap geometry; the expression of volume of droplet is Eq. [12].

$$V_0 = \xi(\theta) r^3 \quad [12]$$

Where,

$$\xi(\theta) = \frac{\pi}{3}\frac{(1-\cos\theta)(\cos\theta+2)}{\sin\theta(\cos\theta+1)} \quad [13]$$

Eq. [9] express the penetration volume of droplet (V_p) as a function of penetration time (t) and contact area radius (r). Thus initial volume (V_0) and total absorption time (τ) can be related as:

$$V_0 = cr^2\sqrt{\tau} \quad [14]$$

Combining Eq. [12] and Eq. [14], total absorption time (τ) can be expressed as:

$$\tau = \frac{\xi^{4/3}(\theta)}{c^2} V_0^{2/3} \quad [15]$$

Where, $$c = \frac{8\pi k}{R^2}\sqrt{\frac{\gamma_{lv} R\cos\theta}{2\mu}}$$

Absorption time is determined by liquid properties (surface tension, viscosity), properties of interaction between the solid material and the liquid (wettability), powder bed structure (pore density, pore size distribution, connectivity) and droplet size. In previous analysis, the absorption time increases with increasing of liquid viscosity and decreasing of porosity (figure 2.14). Also, longer absorption time can be observed in experiments of less wetting materials (figure 2.12). To investigate the effects of droplet size on the absorption time, different size of needles were prepared to make droplets with varying size. Four different droplet size were achieved: 6µl, 9µl, 22cµl and 30.5µl. Blends of 640Rev-90% Lactose, 9% APAP and 1% MgSt was selected as the material. Penetration profile for each droplet size shows in figure 2.22. The relation of droplet size and the absorption time is presented in Eq. [15] and figure 2.23, both of them reveal the absorption time (τ) depend on $V_0^{2/3}$ linearly.

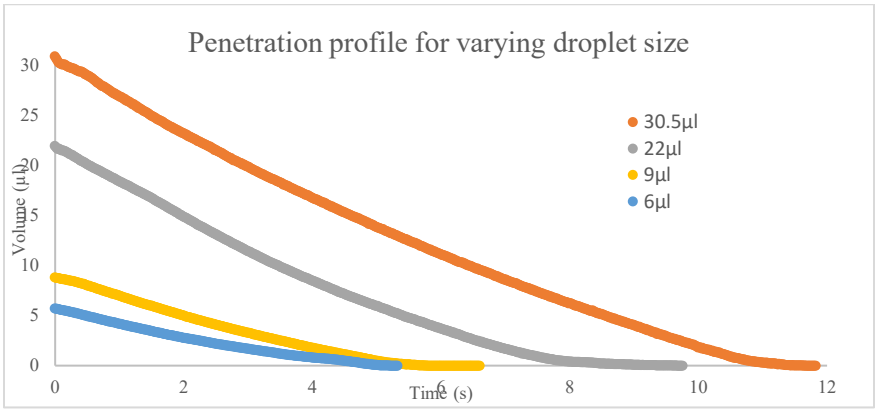

Figure 2.22 Penetration profile with varying droplet size

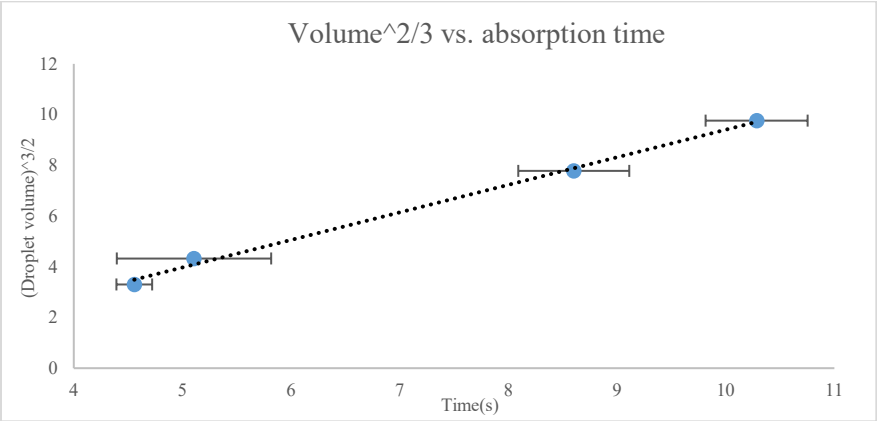

Figure 2.23 Relation of droplet volume with absorption time

2.3.4 Contact angle calculation:

In section 2.3.2, we showed the volume of liquid inside the porous material ($V_p = V_0 - V$) increases as the square root of penetration time. In our case, the contact area between the droplet and the porous material remains constant and the liquid penetrates in the direction perpendicular to the porous surface (Eq. [9]). We plot the graph of penetration volume ($V_p = V_0 - V$) versus square root of time and fit to linear plot (figure2.24). As can be seen in figure 2.12, the slope decreases with increasing blend shear.

A.

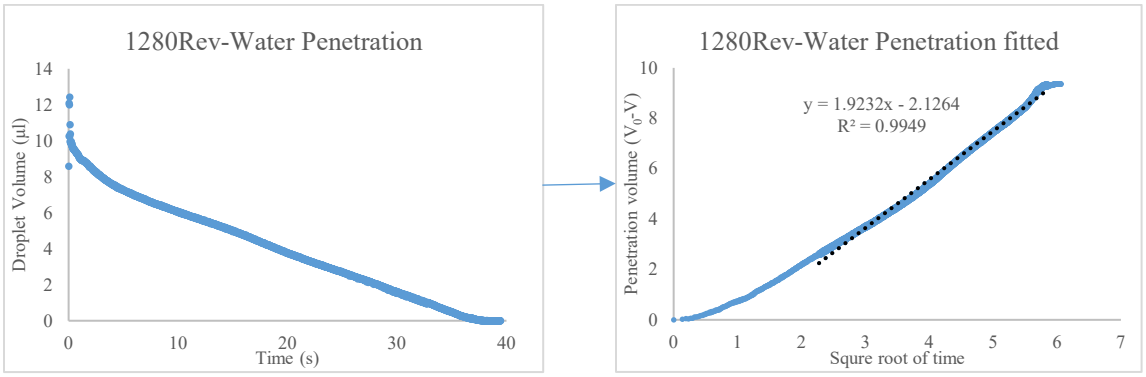

B.

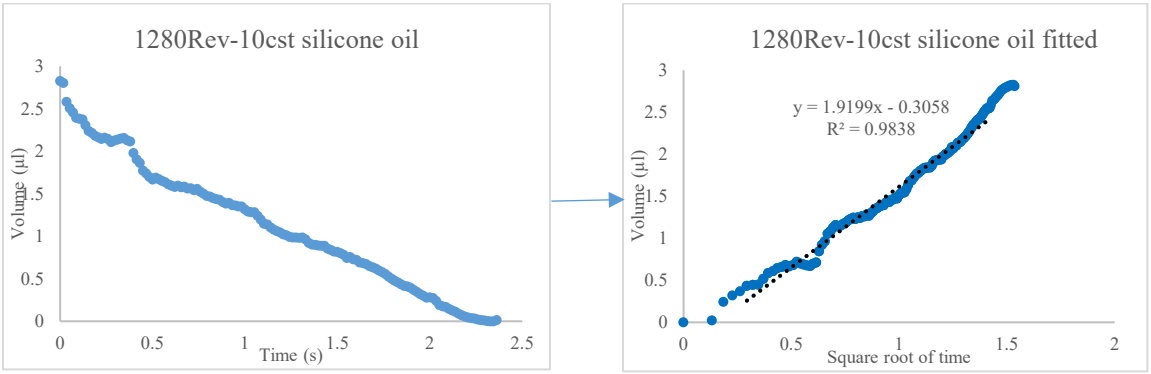

Figure 2.24 Penetration curve fitting for Lactose+APAP+MgSt 1280Rev. A).Water penetration curve fitting B). 10cst silicone oil penetration curve fitting

The slope of fitted line (cr^2 in Eq. [9]) is determined by the cosine of contact angle, the radius of contact area (r_i), the powder bed physical structure and the liquid properties(the indes "w" is used for water and "o" for oil).

$$\frac{S_{water}}{S_{silicone\cdot oil}} = \frac{c_w r_w^2}{c_o r_o^2} = \frac{\sqrt{\frac{\gamma_w \cos\theta_w}{\mu_w}} \cdot r_w^2}{\sqrt{\frac{\gamma_o \cos\theta_o}{\mu_o}} \cdot r_w^2} \qquad [16]$$

By measuring the slope of water penetration; the slope of the silicone oil penetration, which the contact angle is zero; and the radius of the contact area of both water droplets and silicone oil droplets, contact angle between water and blends can be calculated as:

$$\frac{\cos\theta_w}{\cos\theta_o} = \left(\frac{S_w}{S_o}\right)^2 \cdot \left(\frac{r_o}{r_w}\right)^4 \left(\frac{\gamma_o \mu_w}{\gamma_w \mu_o}\right) \qquad [17]$$

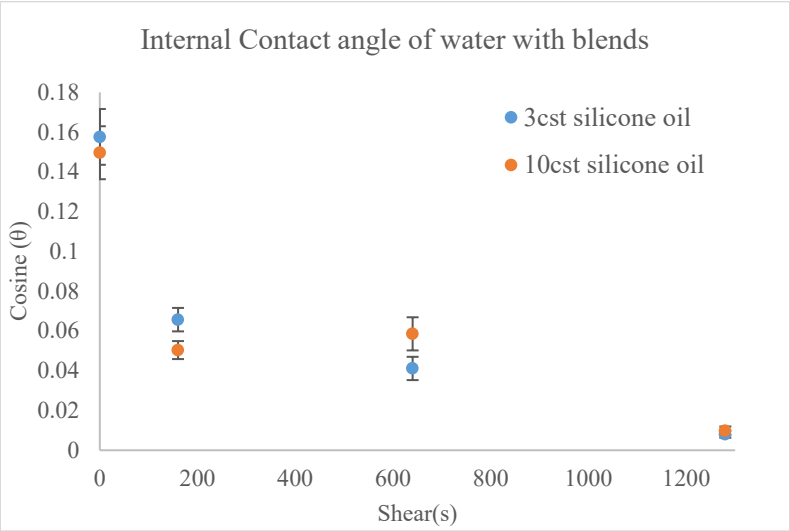

Figure 2.25 Contact angle of water with blends

Cosine of contact angle of four blends were calculated and shown in figure 2.25. As the shear level increasing, cosine of contact angle decreases. From 0Rev to 160Rev, big change of contact angle was found. While, 160Rev and 640Rev blends didn't show much difference. Largest contact angle was shown in 1280Rev blends due to over lubrication. Moreover, the results of both 3cst and 10cst silicone oil are similar. We are going to use 10cst for the rest of the work.

The cosine of contact angle of pure Lactose and blends of Lactose+APAP are also calculated as table 2-3.

Table 2-3 Contact calculation of Lactose and blends without MgSt

Material	Contact angle (cosθ)
Lactose	0.061178
90% Lactose, 10% APAP 0Rev	0.046863
90% Lactose, 10% APAP 1280Rev	0.042502

It is surprising that the dynamic contact angle of pure Lactose and blend without MgSt are smaller than that of 0Rev blends with 1% MgSt, which is different with our expected. Experiments for more materials are needed to explain it. We propose several possible reasons leads to the error of contact angle calculation:

A.) As said before, we plot the penetration volume versus square root of time and fit it to linear plot. The whole penetrating curve of Lactose and blends without MgSt present linear behavior. However, the whole curve of 0Rev blends with MgSt is not linear (figure 2.26), which means different part of curve present different slope. In previous calculation, we fitted the end part of the curve, where the linear part is longer. However, we can not confidently regard the slope of end part as cr^2 of Eq. [14]. In addition, with shear level increasing, longer part of curve represent the same slope. From figure 2.24 A, the whole curve of 1280Rev blends is perfect linear plot with just a very short initial part, where the slope is different with others.

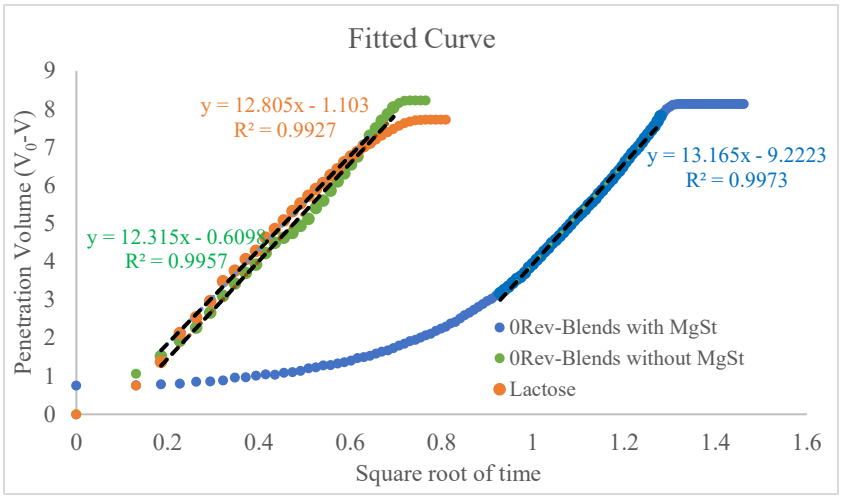

Figure 2.26 Fitted penetrating curve for Lactose, Lactose+APAP, 0Rev of Lactose+APAP+MgSt

We can related this non-linear behavior with heterogeneity of powder beds. The powder beds of pure lactose is the homogeneous powder beds. Also, we can regard the powder bed

of blends of 90% Lactose+10% APAP as homogeneous powder beds because 90% of powder bed is Lactose. Thus, whole curve of Lactose and blends without MgSt are linear plot. Due to the existence of MgSt (particle size is very small), powder beds of 0Rev blends with MgSt have the highest heterogeneity. But, as the shear level increasing, powder beds are trending to homogeneous. Therefore, the whole curves of blends with higher shear level present longer linear part.

B).We propose the waiting phase affects the penetration of liquid. The waiting phase may be one of the reasons that contribute to the non-linear function of penetration time versus square root of time as well.

C). In section 2.3.1, we introduced the effect of roughness on the contact angle that was studied by Wenzel. The silicone oil analysis can help us remove the effect of the porosity and the connectivity on the contact angle calculation. However, it cannot remove the effect of powder bed roughness on contact angle calculation. It is impossible that different powder beds have identical structure (roughness), even they are made of same blends. Hence, ignoring the effect of roughness probably leads to the error more or less. For pure Lactose and blends without MgSt (Lactose + APAP), the total water penetration is very fast (less than 1s). Thus, the effect from roughness may not be captured. Roughness of the powder bed depends on the particle size and the particle shape. Thus, to investigate the effect of roughness, we should change the particle size and the particle shape and investigate how roughness of powder affects the liquid penetration.

Therefore, more work should be done to investigate this unexpected result in the future.

2.4 conclusion

We studied the penetration behavior for blends with and without MgSt. The volume of droplet versus time have been plotted. Droplet penetration experiments of water and 10cst silicone oil for both pure Lactose and Lactose+APAP were performed. The results show that, as expected, liquid penetrates into powder beds made of Lactose or Lactose+APAP immediately due to high water wettability of blends. Furthermore, shear level doesn't alert wettability of blends without MgSt.

As hydrophobic lubricant, MgSt affects the water wettability of blends during the lubricating process. Since small hydrophobic particles (MgSt) coat on the surface of large hydrophilic particles (Lactose and possibly APAP), hydrophilic particles will form hydrophobic surface. Thus, material with same formulation but different properties is generated in the lubricating process. In this thesis, blends with same formulation but different shear condition (shear strain level) was prepared to investigate the droplet penetration behavior, and three phase was observed in the water penetration process: bouncing, waiting, penetrating. Water penetration behavior in the penetrating phase relate to wettability of blends dominantly. Blend with higher shear level presents longer penetrating phase, which reveals less wettable material is obtained as the shear level increasing. Determined by the powder bed structure (porosity, pore size distribution and connectivity) mainly, penetration behavior of silicone oil was also investigated to remove the effect of the pore geometry in penetrating phase. Due to smaller porosity, blends with higher shear level represent longer penetration time of silicone oil.

The model of capillary penetration of droplet into the porous material has been reviewed. Both the penetration model and results of experiments reveal that the penetration behavior is dominated by the wettability of material, viscosity and surface tension of liquid, porosity and pores size of powder bed and droplet size. Investigation shows how these effects contribute to the absorption time (Eq. [15]). Longer absorption time can be approached in the experiments with higher viscosity of liquid, smaller porosity of powder bed, lower wettability of material, and larger droplet size. Combining the penetration behavior of water and silicone oil, the contact angle between blends and water, which represents the wettability of blends, can be calculated.

Chapter3 Swelling of pharmaceutical tablets in contact with water

As we mentioned in Chapter 1, Swelling of the tablets plays a crucial role in the tablets disintegration because it links to force development and water uptake. To understand swelling dynamics and water uptake mechanisms during the tablets swelling, we established quantitatively measurements in which we can plot the swelling profile and water uptake profile. In addition, we can calculate the swelling rate and water uptake rate from the swelling profile and the water uptake profile. In this chapter, three formulation with varying percentage of Lactose and Avicel were prepared to investigate swelling behavior with formulation. For each formulation, tablets with different compaction forces were made to approach how compaction affects swelling behavior. The results show that both swelling profile and water profile present two different behaviors (linear behavior and non-linear behavior) with compaction, which reveal two possible water uptake mechanisms in swelling process. In the end, the swelling rate and the water uptake rate were calculated from the swelling profile and the water uptake profile, from which, we observed both of them are non-monotonic with formulation and compaction. Although, Barry and Ridout reported a non-monotonic behavior of the tablets disintegration with compaction in 1950[21]. They never related to different water uptake mechanisms. In our investigation, we postulate the different water uptake mechanisms are responsible for the non-monotonic swelling behavior with compaction and the particle-particle interaction is responsible for non-monotonic swelling behavior with formulation.

3.1 Material and Methods

3.1.1 Materials and tableting.

We use Microcrystalline Cellulose (Avicel, PH102) and monohydrated α-Lactose as excipients; semifine Acetaminophen (APAP) as the active ingredient; and Magnesium Stearate (MgSt) as the lubricant. Microcrystalline cellulose (Avicel) can swell very fast but cannot dissolve into water. Lactose can dissolve into water easily. Thus, it will be possible to investigate the effect of formulation on swelling dynamics by varying the concentration of Avicel and Lactose. Three different formulations with varying concentration of Avicel and Lactose were performed: 10% Avicel 80% Lactose 9% APAP 1% MgSt, 45% Avicel 45% Lactose 9% APAP 1% MgSt, and 80% Avicel 10% Lactose 9% APAP 1% MgSt. All formulations were mixed in a 4-quart V-blender (figure 2.4). Avicel, Lactose and APAP were fed into V-blender for 15 minutes blending. Then, MgSt was added into V-blender and blending procedure continue for another 2mins.

Blends were tableted in a direct compaction press Presster^{TM} (Metropolitan Computer Corporation) (figure 3.1). The Presster^{TM} is a press simulator that can simulate (or synonym) a wide variety of compaction machines used in the pharmaceutical industry. The model of Fette II 2090 IC at 20RPM was selected in our case. A 10mm diameter punch with flat surface was used and the compaction force was varied between 4KN and 24KN (4KN, 8KN, 12KN, 16KN, 20KN and 24KN) giving a compaction spectrum between 50MPa and 300MPa. The mass of each tablet was fixed as 350mg. The mass of each tablets was measured by an OHAUS balance and the compaction force of each tablets can be read from the Presster^{TM}.

Figure 3.1 Directed compaction presster™

3.1.2 Porosity of tablets

Porosity of tablets was calculated by:

$$\varepsilon = 1 - \frac{m}{\rho V} \quad [18]$$

Where, m is the mass of tablet, V is the volume of tablet, and ρ is the true density of blends which can be expressed by Eq. [19].

$$\rho = f_{Lactose}\rho_{Lactose} + f_{Avicel}\rho_{Avicel} + f_{APAP}\rho_{APAP} + f_{MgSt}\rho_{MgSt} \quad [19]$$

$\rho_{Lactose}$, ρ_{Avicel}, ρ_{APAP} and ρ_{MgSt} are corresponding to density of Lactose (1.5588 g/cm^3), Avicel (1.5617 g/cm^3), APAP (1.2994 g/cm^3) and MgSt (1.04 g/cm^3)[29]. $f_{Lactose}$, f_{Avicel}, f_{APAP} and f_{MgSt} represent the mass fraction of each component. Assuming tablet is cylindrical shape, the volume of tablets was obtained by measuring their thickness and diameter.

Porosity of tablets with different formulation and compaction force is shown as figure 3.2.

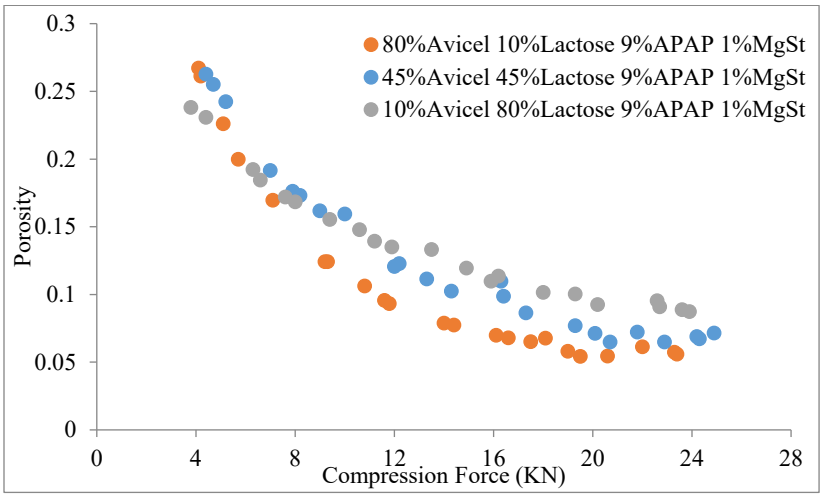

Figure 3.2 porosity of tablets with compaction

Compression force is one of the main factors that control the performance of tablets. As expected, tablets have lower porosity with increasing compression force. Furthermore, Avicel is a polymeric material with excellent compressibility and it is more easily deformed than lactose. At high compression forces (>8KN), tablets with larger percentage of Avicel result in lower porosity. We also observe that for compaction force above16KN, porosity of the tablets does not change significantly with compaction.

3.1.3 Tablet swelling technique

To measure the volume of tablets swelling and the mass of water uptake with time, experiments were designed in which one of the tablets surface put in contact with water instead of completely immersing tablets into the water. This design has at least four advantages with respect to immersing the tablet directtly into the solvent: A). Tablets can keep their integrity during swelling and would not break into pieces. B). Water uptake can be easily measured. C). It is easy to follow the swelling of the tablet by optical means as the medium surrounding the tablet is not disturbed. D). Swelling is closer to a 1D problem so results can be more easily interpreted. The setup for experiments is shown in figure 3.3.

Tablets were deposited on a tablet holder, which is a metallic mesh with a central hole of 7mm diameter. The tablet holder was moved down until the tablet touches water and swelling starts. Swelling process was captured using a CCD camera (GimaGo434C, NET Gmbh) and a video recorder (FGControl). Frame rate of camera was set to 1 frame/s. The mass of water uptake was recorded using the OHAUS Balance Talk for each second as well. Camera and OHAUS Balance Talk were connected to a computer.

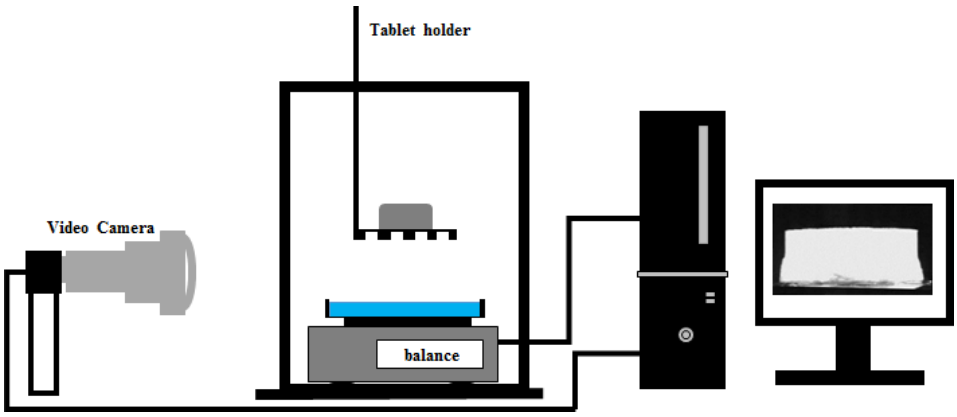

Figure 3.3 Swelling experiments setup

All the videos were converted to sequence of stacks in Avidemux. Stacks were opened in ImageJ. An automatic threshold was set and the images were binarized. Then, using a similar macro as described in chapter 2, volume of tablet in each image can be calculated assuming the tablet is axi-symmetric.

3.2 Results and Discussion

3.2.1 Swelling behavior and discussion

Some images in the tablets swelling processes can be seen in figure 3.4. Pictures were taken before the swelling process starts, during swelling and after swelling has finished. When the tablet touches the water surface, liquid penetrates into the tablet and the swelling

process starts. The swelling front propagates vertically and the volume of the tablets increases.

Figure 3.4 Swelling Processes of 80% Avicel, 45% Avicel, 10% Avicel and 4KN, 8KN, 16KN, 24KN.

For a given compaction force, tablets with 45% Avicel swells faster than tablets made of either 80% or 10% Avicel. For example, considering 8KN tablets, those made of 45% Avicel need 19s for swellings. The swelling time for tablets of 80% Avicel and 10% Avicel were 34s and 39s respectively. Longer swelling time was found for tablets with higher compaction. For 80% Avicel tablets, swelling time of tablets made by 8KN was 34s. Tablets made by 24KN would need 390s to swell completely. However, we found the

swelling process of 4KN tablets take longer time than 8KN tablets, which means the swelling gives non-monotonic behavior with compaction.

3.2.2 Swelling profile:

The volume of tablet and the mass of water uptake as function of time are shown in figure 3.5. Both volume and mass profile give similar behavior. Profiles with same formulation and different compaction condition were compared in the same plot.

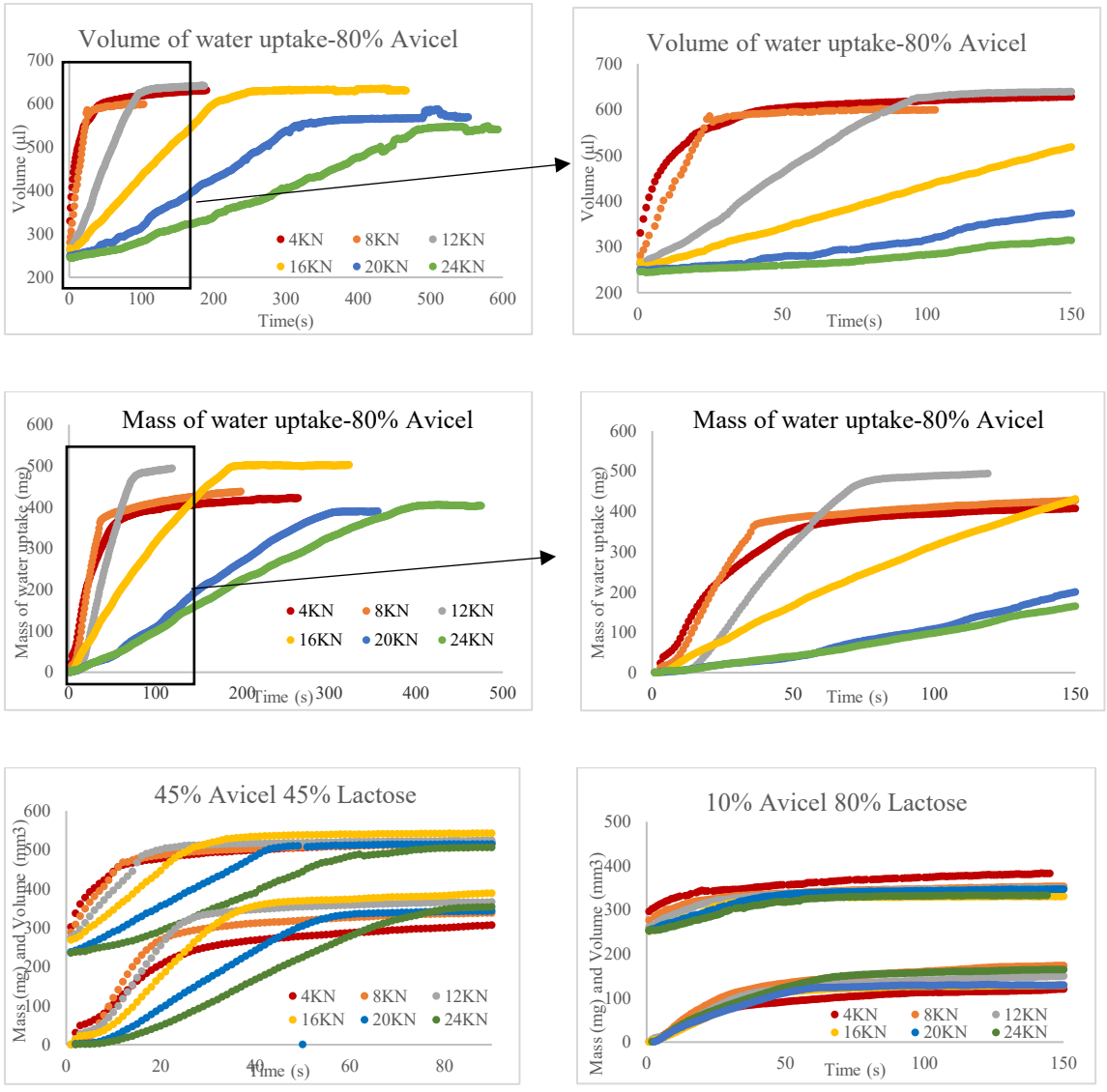

Figure 3.5 Swelling profile and water uptake profile

In all the curves except for 4KN tablets (tablets with high porosity), the volume of the tablets and the mass of water uptake increase with time linearly at short time. At the end, of curves, tablets were saturated by water and both volume and mass do not change in time. This linear behavior is attributed to the swelling of Avicel particles, which we will discuss in section 3.2.4. Both curves of 80% Avicel tablets and 45% Avicel tablets represent similar behavior with compaction. However, due to low Avicel concentration in tablets, 10% Avicel tablets didn't shows the swelling behavior clearly, meaning the volume of tablets and the mass of water uptake didn't change much (comparing with the 45% Avicel swelling and the 80% Avicel swelling).

The second observation in experiments is water uptake lags behind volume swelling, which can be revealed by looking into the mean density of the tablets during swelling processes (figure 3.6). Due to faster volume change than water uptake, the mean density initially decreases from its initial value. When water penetrates into the Avicel particles, the liquid restructure H-bonds present in Avicel particles and creates more spaces for water uptake. The volume of the Pores inside the tablets increase. Also, as the swelling front reaches to the upper surface of the tablets, the swelling process of tablet stops, but the water uptake continues. As a result, the mean density increases until it reaches its final value. The mean density curves for 10% Avicel tablets do not decrease much due to the swelling of the tablets is not significant. The mean density of 20KN and 24KN tablets with 80% Avicel increases initially from 1.4mg/mm^3 to 1.5mg/mm^3 and then decreases. This means that the liquid penetrates into tablets first and the swelling lags behind. We propose a possible reason that contributes to this phenomenon: The bonding force between particles increases with compaction force. It is not surprising that Avicel particles of the highly compressed

tablet take longer time to swell. In this case, Water uptake by the capillary penetration is a little faster than by swelling initially. However, when the swelling starts, the swelling of particles creates space for water uptake, which gives faster water uptake later. Thus, mean density decrease after some time. Also, the mean density of 24KN tablet with 10% Avicel increase from 1.4mg/mm^3 to 1.5mg/mm^3 during swelling process. In this case, we propose Avicel particles withstand more resistance for swelling due to high compaction force. Moreover, the total swelling of tablets is very small, which means swelling particle doesn't create too much space for faster water uptake, Thus, the mean density for this particular case increases in swelling process.

Figure 3.6 Mean density of tablets in swelling process

3.2.3 Final swelling:

Both the maximum volume of tablet and the maximum mass of water uptake after swelling can be calculated from the swelling profile (figure 3.7). All tablets with same formulation achieve similar final swelling state, which means the similar volume of tablets and the similar mass of water uptake. Total swelling doesn't depend on the compression force. Moreover, since most of the swelling comes from the Avicel, it make sense that tablets with higher Avicel concentration achieve larger final volume and more water uptake.

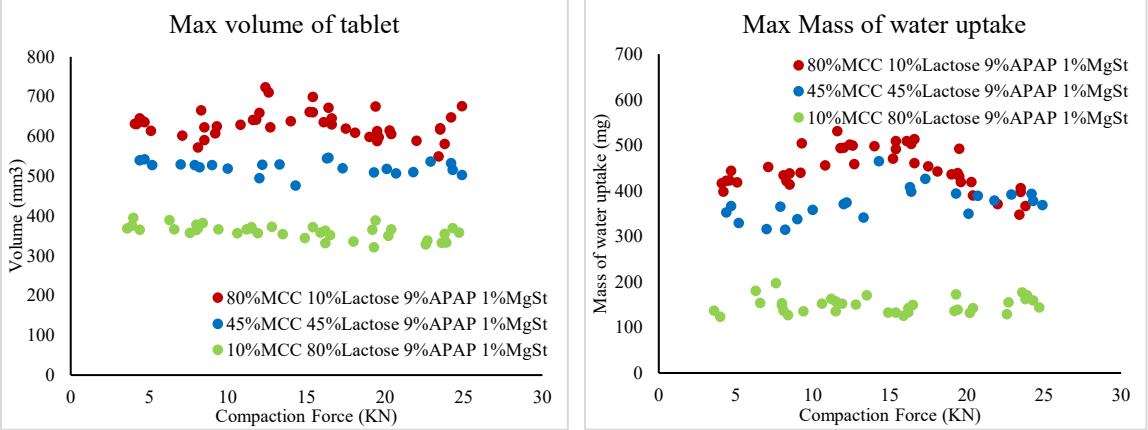

Figure 3.7 Final swelling

We are also interested in the swelling of individual Avicel particle. The average swelling of individual Avicel particle can be calculated as Eq. [20]

$$\phi = \frac{V_{final} - V_{initial}}{V_{Avicel}} \qquad [20]$$

Where, $V_{Avicel} = m_{Avicel} / \rho_{Avicel}$ represents total volume of Avicel in a tablet.

Swelling ratio (Φ) represent volume change of each Avicel particle in swelling process. And, the swelling ratio versus concentration of Avicel is shown in figure 3.8.

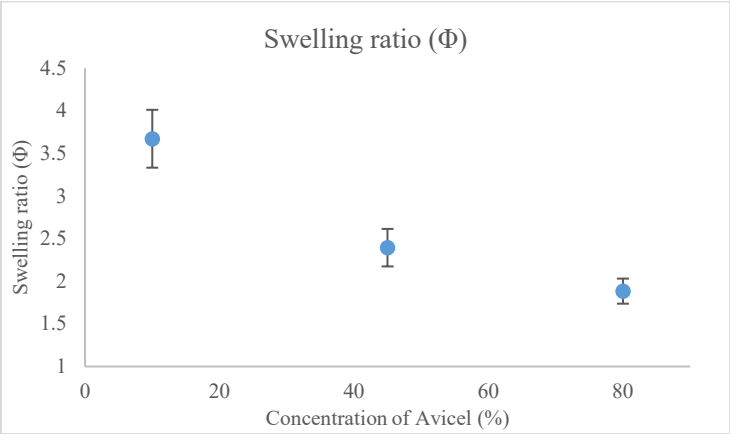

Figure 3.8 Individual particle swelling

Average swelling of each Avicel particle decreases with Avicel concentration. Mean volume of individual Avicel particle in 10% Avicel tablets is 3.7 times larger after swelling. While, in 45% Avicel tablets, it is 2.4 times larger and 1.9 times larger in 80% Avicel tablets. Due to interaction between swollen particles, Avicel particles doesn't swell completely for high Avicel concentration tablets. In summary, the total swelling of tablets with higher Avicel concentration is much bigger, but the individual Avicel particle doesn't swell too much.

3.2.4 Swelling dynamic

In section 3.2.2, the swelling profile and the water uptake profile were performed and we observed two different behavior: non-linear and linear. To understand swelling dynamic, we calculate swelling rate and water uptake rate. Above 8KN, the swelling and the water uptake give linear behavior. Rate of swelling and water uptake are defined as slope of the linear part of swelling curves. While, non-linear behavior was observed in curves of tablets below 8KN. For this case, rate of the swelling and the water uptake can be calculated as the mean rate of volume and water uptake increase at 90% total swelling ($=(90\%V_{\max}-V_0)/t_{90\%V_{\max}}$).

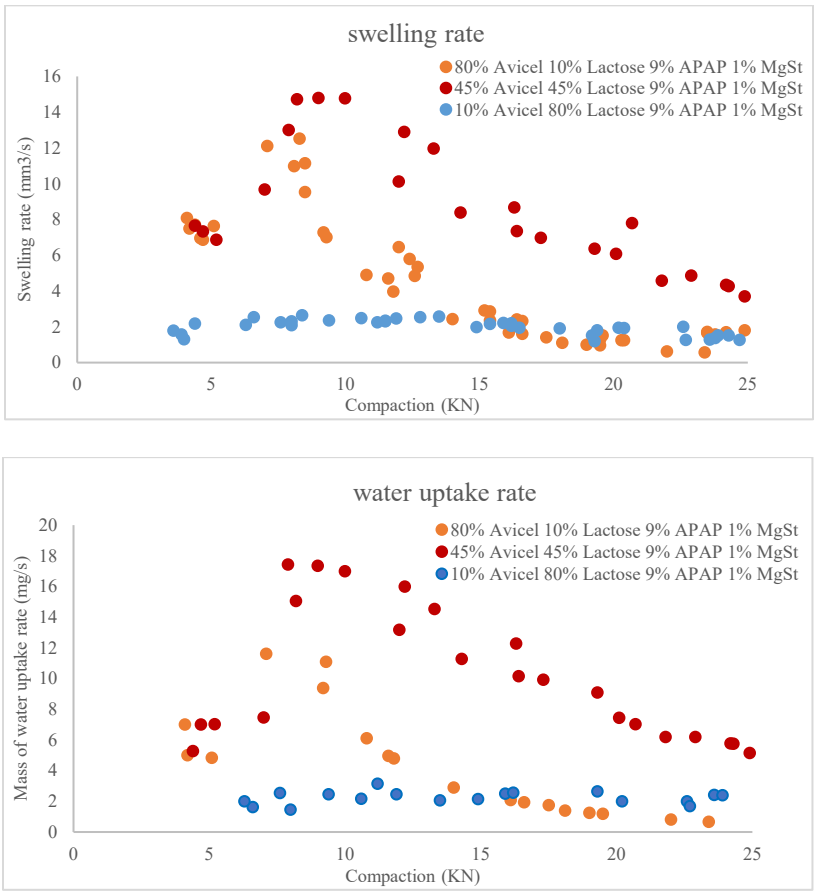

Figure 3.9 Swelling rate and water uptake rate

Both swelling rate (mm^3/s) and water uptake rate (mg/s) present similar behavior with the compaction force. The rate obtained for tablets compressed below 8KN is much smaller than the ones obtained at 8KN. Then, the rate decrease with the compaction, which means the swelling rate is non-monotonic with compaction. Tablets made by formulation of 10% Avicel 80% Lactose 9% APAP 1% MgSt didn't show clear swelling process. Thus, swelling rate and water uptake rate is low and the non-monotonic behavior with compaction is not observed. Furthermore, swelling rate and water uptake rate of tablets made of 45% Avicel is larger than that of 80% Avicel and 10% Avicel. In other words, swelling behavior is non-monotonic with formulation as well.

We mentioned the corollary of Caramella in chapter1: the swelling force does not increase with the amount of disintegrants monotonically. In our case, during the swelling process of 80% Avicel tablets, the swelling of each Avicel particle is hindered by surrounding particles due to high Avicel concentration. It has to overcome more resistance for swelling. From figure 3.8, we concluded that the individual Avicel particle didn't swell completely in 80% Avicel case. Thus, it is possible that the swelling rate of the 80% Avicel tablet is not high even if the amount of Avicel is large. For 10% Avicel tablets, due to small concentration of Avicel, the amount of swelling was not much and the spaces for water uptake were limited. Thus, they showed low swelling rate and water uptake rate. Tablets made of 45% Avicel give the highest swelling efficiency. The swelling of each Avicel particle in these tablets doesn't have much resistance from surrounding particles probably. Moreover, bonding annihilation (Lactose) is faster than swelling (MCC). But, without swelling, water takes more time to reach inner grains. Swelling opens more channels for fast water uptake. Therefore, the swelling behavior is non-monotonic with formulation.

The non-monotonic behavior with compaction may relates to two different water uptake mechanisms. Since Avicel is polymeric material, the hydrogen bond generates in Avicel during compaction process. When tablets touch water, liquid penetrates into tablets and invades the void space between particles (or pores). When in contact with the particles, water restructures H-bond and leads to swelling. Swelling front propagates at constant speed[37]. Contacts increase with the compaction, but also the higher compaction leads to more resistance to swelling. The linear swelling behavior for tablets with higher compaction force (above 8KN) reveals the constant speed of swelling propagation and particles swelling mechanism is dominant. On the other hand, liquid penetrated through

inter-particle pores by capillary force, which follows Washburn kinetics[5] (penetration front go up as square root of time). Porosity and pores size decide penetration rate, and both of them decrease with compaction. Therefore, longer penetration time is needed for tablet with higher compaction. The non-linear curves of 4KN tablets may reveal that water go through tablets following the Washburn kinetics mainly. Two water uptake mechanisms are shown in figure 3.10.

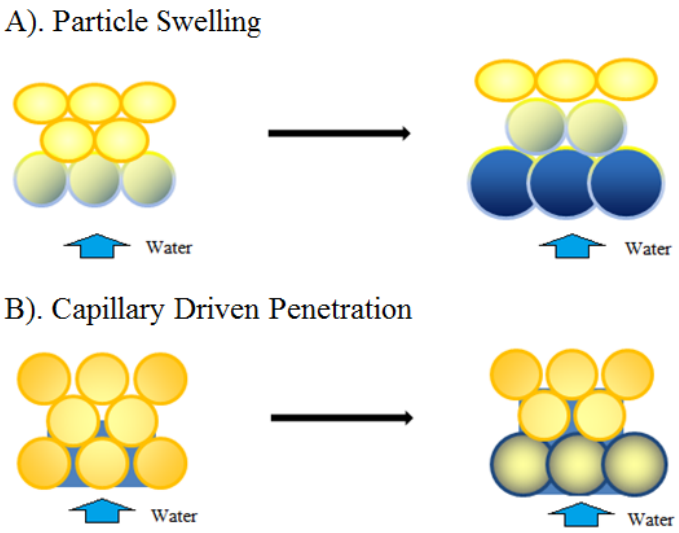

Figure 3.10 Two mechanism for water uptake.

3.3 Conclusion

In our investigation, the swelling profile of highly compacted tablets presents linear swelling behavior. And, the swelling profile of tablet with low compaction (below 8KN) is non-linear. All compacted tablets made of same formulation achieve similar final swollen state, which means the total swelling doesn't depends on compaction. Total swelling of tablets increases with Avicel concentration. However, because of interaction between swollen particles, amount of swelling per particle decrease with Avicel concentration. Swelling dynamics were measured from swelling profile and water uptake

profile, from which, we find the swelling rate and the water uptake rate is non-monotonic with compaction and formulation. In our case, 8KN tablets, where the porosity of all tablets is more or less 0.17, give the fastest swelling. Also, 45% Avicel tablets swells faster than 10% Avicel tablets and 80% Avicel tablets. We propose capillary penetration and particle swelling coupled in the water uptake process, which leads to the non-monotonic behavior with compaction. For low compaction (below 8KN), water uptake dynamics is dominated by capillarity (inter-particle pores). Water penetrates faster through inter-particle pores. The swelling front propagate but swelling is not complete. When the front reach to the upper surface of tablet, the swelling is continuous in a period of time. For high compaction, water uptake dynamics is dominated by swelling. Swelling open channels for water to penetrate into tablets, meaning that it is needs for water penetration. Particles swelling is completed during propagating of swelling front.

Reference

[1] Perrie, Y. and T. Rades (2012). FASTtrack Pharmaceutics: Drug Delivery and Targeting, Pharmaceutical Press.
[2] Jivraj, M., et al. (2000). "An overview of the different excipients useful for the direct compression of tablets." Pharmaceutical science & technology today **3**(2): 58-63.
[3] Rowe, R. C., et al. (2009). Handbook of pharmaceutical excipients, Pharmaceutical press London.
[4] Thoorens, G., et al. (2014). "Microcrystalline cellulose, a direct compression binder in a quality by design environment—A review." International journal of pharmaceutics **473**(1): 64-72.
[5] Washburn, E. W. (1921). "The dynamics of capillary flow." Physical review **17**(3): 273.
[6] Caramella, C., et al. (1984). "The role of swelling in the disintegration process." International Journal of Pharmaceutical Technology & Product Manufacture **5**: 1-5.
[7] Caramella, C., et al. (1990). "Characterization of particle swelling of materials of pharmaceutical interest." Particle & Particle Systems Characterization **7**(1‐4): 131-135.
[8] Caramella, C., et al. (1988). "A physical analysis of the phenomenon of tablet disintegration." International journal of pharmaceutics **44**(1): 177-186.
[9] Guyot-Hermann, A. and D. J. Ringard (1981). "Disintegration mechanisms of tablets containing starches. Hypothesis about the particle-particle repulsive force." Drug Development and Industrial Pharmacy **7**(2): 155-177.
[10] Caramella, C., et al. (1986). "Water uptake and disintegrating force measurements: towards a general understanding of disintegration mechanisms." Drug Development and Industrial Pharmacy **12**(11-13): 1749-1766.
[11] Melia, C. and S. Davis (1989). "Review article: Mechanisms of drug release from tablets and capsules. 2. Dissolution." Alimentary pharmacology & therapeutics **3**(6): 513-525.
[12] Llusa, M., et al. (2010). "Measuring the hydrophobicity of lubricated blends of pharmaceutical excipients." Powder Technology **198**(1): 101-107.
[13] Pingali, K., et al. (2011). "Evaluation of strain-induced hydrophobicity of pharmaceutical blends and its effect on drug release rate under multiple compression conditions." Drug Development and Industrial Pharmacy **37**(4): 428-435.
[14] Mehrotra, A., et al. (2007). "Influence of shear intensity and total shear on properties of blends and tablets of lactose and cellulose lubricated with magnesium stearate." International journal of pharmaceutics **336**(2): 284-291.
[15] Middleman, S. (1995). Modeling axisymmetric flows: dynamics of films, jets, and drops, Academic Press.
[16] Hapgood, K. P., et al. (2002). "Drop penetration into porous powder beds." Journal of Colloid and Interface Science **253**(2): 353-366.
[17] McHale, G., et al. (2005). "Water‐repellent soil and its relationship to granularity, surface roughness and hydrophobicity: a materials science view." European Journal of Soil Science **56**(4): 445-452.
[18] Emady, H. N., et al. (2013). "A regime map for granule formation by drop impact on powder beds." AIChE Journal **59**(1): 96-107.

[19] Oostveen, M. L., et al. (2015). "Quantification of powder wetting by drop penetration time." Powder Technology **274**: 62-66.
[20] Nguyen, T., et al. (2009). "Drop penetration time in heterogeneous powder beds." Chemical Engineering Science **64**(24): 5210-5221.
[21] Berry, H. and C. Ridout (1950). "THE PREPARATION OF COMPRESSED TABLETS: Part III.—A Study of the Value of Potato Starch and Alginic Acid as Disintegrating Agents." Journal of Pharmacy and Pharmacology **2**(1): 619-629.
[22] Adolfsson, Å. and C. Nyström (1996). "Tablet strength, porosity, elasticity and solid state structure of tablets compressed at high loads." International journal of pharmaceutics **132**(1): 95-106.
[23] Faroongsarng, D. and G. E. Peck (1994). "The swelling & water uptake of tablets iii: moisture sorption behavior of tablet disintegrants." Drug Development and Industrial Pharmacy **20**(5): 779-798.
[24] List, P. and U. Muazzam (1979). "Swelling the Driving Force in Tablet Disintegration." Pharm. Ind **41**: 459-464.
[25] Colombo, P., et al. (1981). "Disintegrating force and tablet properties." Drug Development and Industrial Pharmacy **7**(2): 135-153.
[26] Caramella, C., et al. (1987). "Tablet disintegration update: the dynamic approach." Drug Development and Industrial Pharmacy **13**(12): 2111-2145.
[27] Catellani, P., et al. (1989). "Tablet water uptake and disintegration force measurements." International journal of pharmaceutics **51**(1): 63-66.
[28] Colombo, P., et al. (1984). "Disintegrating force as a new formulation parameter." Journal of pharmaceutical sciences **73**(5): 701-705.
[29] S. M. Razavi, G. C., G.Drazer, A. M. Cuitiño ((2015) (Submitted for publication)). "Toward predicting tensile strength of pharmaceutical tablets by ultrasound measurement in continuous manufacturing."
[30] "ImageJ." from http://imagej.nih.gov/ij/.
[31] Wenzel, R. N. (1936). "Resistance of solid surfaces to wetting by water." Industrial & Engineering Chemistry **28**(8): 988-994.
[32] Cassie, A. and S. Baxter (1944). "Wettability of porous surfaces." Transactions of the Faraday Society **40**: 546-551.
[33] Marmur, A. (1988). "The radial capillary." Journal of Colloid and Interface Science **124**(1): 301-308.
[34] Denesuk, M., et al. (1993). "Capillary penetration of liquid droplets into porous materials." Journal of colloid and interface science **158**(1): 114-120.
[35] Scheidegger, A. E. (1958). "The Physics of Flow Through Porous Media." Soil Science **86**(6): 355.
[36] Markicevic, B., et al. (2009). "Infiltration time and imprint shape of a sessile droplet imbibing porous medium." Journal of Colloid and Interface Science **336**(2): 698-706.
[37] Alfrey, T., et al. (1966). Diffusion in glassy polymers. Journal of Polymer Science Part C: Polymer Symposia, Wiley Online Library.